

### Public Domain Mark 1.0 Universal

This work was written as part of one of the author's official duties as an Employee of the United States Government and is therefore a work of the United States Government. In accordance with 17 U.S.C. 105, no copyright protection is available for such works under U.S. Law.

Access to this work was provided by the University of Maryland, Baltimore County (UMBC) ScholarWorks@UMBC digital repository on the Maryland Shared Open Access (MD-SOAR) platform.

### **Please provide feedback**

Please support the ScholarWorks@UMBC repository by emailing [scholarworks-group@umbc.edu](mailto:scholarworks-group@umbc.edu) and telling us what having access to this work means to you and why it's important to you. Thank you.

## Remote sensing in BOREAS: Lessons learned

J.A. Gamon<sup>a</sup>, K.F. Huemmrich<sup>b,\*</sup>, D.R. Peddle<sup>c</sup>, J. Chen<sup>d</sup>, D. Fuentes<sup>a</sup>, F.G. Hall<sup>b</sup>,  
J.S. Kimball<sup>e</sup>, S. Goetz<sup>f</sup>, J. Gu<sup>g</sup>, K.C. McDonald<sup>h</sup>, J.R. Miller<sup>i</sup>, M. Moghaddam<sup>h</sup>, A.F. Rahman<sup>j</sup>,  
J.-L. Roujean<sup>k</sup>, E.A. Smith<sup>l</sup>, C.L. Walthall<sup>m</sup>, P. Zarco-Tejada<sup>n</sup>, B. Hu<sup>i</sup>, R. Fernandes<sup>o</sup>, J. Cihlar<sup>o</sup>

<sup>a</sup>Center for Environmental Analysis (CEA-CREST) and Department of Biological Sciences, California State University Los Angeles, Los Angeles, CA, USA

<sup>b</sup>Joint Center for Earth Systems Technology, University of Maryland Baltimore County, Baltimore, MD, USA

<sup>c</sup>Department of Geography, University of Lethbridge, Lethbridge, Alberta, Canada

<sup>d</sup>Department of Geography, University of Toronto, Toronto, Ontario, Canada

<sup>e</sup>The University of Montana, School of Forestry/NTSG, Missoula, MT, USA

<sup>f</sup>The Woods Hole Research Center, Woods Hole, MA, USA

<sup>g</sup>Department of Meteorology, The Florida State University, Tallahassee FL, USA

<sup>h</sup>Jet Propulsion Laboratory, Pasadena, CA, USA

<sup>i</sup>Department of Physics and Astronomy, York University, Toronto, Ontario, Canada

<sup>j</sup>Department of Geography, Ball State University, Muncie, IN, USA

<sup>k</sup>Meteo-France CNRM/GMME/MATIS, Toulouse Cedex, France

<sup>l</sup>Code 912, NASA Goddard space flight Center, Greenbelt, MD, USA

<sup>m</sup>Hydrology and Remote Sensing Laboratory, USDA-Agricultural Research Service, Beltsville, MD, USA

<sup>n</sup>Universidad de Valladolid, Palencia, Spain

<sup>o</sup>Canada Centre for Remote Sensing, Ottawa, Ontario, Canada

Received 30 May 2002; received in revised form 20 August 2003; accepted 23 August 2003

### Abstract

The Boreal Ecosystem Atmosphere Study (BOREAS) was a large, multiyear internationally supported study designed to improve our understanding of the boreal forest biome and its interactions with the atmosphere, biosphere, and the carbon cycle in the face of global climate change. In the initial phase of this study (early 1990s), remote sensing played a key role by providing products needed for planning and modeling. During and after the main BOREAS field campaigns (1994 and 1996), innovative remote sensing approaches and analyses expanded our understanding of the boreal forest in four key areas: (1) definition of vegetation structure, (2) land-cover classification, (3) assessment of the carbon balance, and (4) links between surface properties, weather, and climate. In addition to six BOREAS special issues and over 500 journal papers, a principal legacy of BOREAS is its well-documented and publicly available database, which provides a lasting scientific resource and opportunity to further advance our understanding of this critical northern biome.

© 2003 Elsevier Inc. All rights reserved.

**Keywords:** Boreal forest; Remote sensing; Carbon cycle; Land cover

### 1. Introduction

The northern latitude boreal forest biome is a critical component of the Earth's climate system (Sellers et al., 1997). Its very large areal extent exerts a significant impact on the Earth's energy balance and the associated surface-atmosphere exchanges of radiation, heat, water, momentum,

and carbon dioxide. The main goals of the Boreal Ecosystem Atmosphere Study (BOREAS) were to improve our understanding of the structure and function of the boreal forest biome and to clarify its interaction with climate and its role in the carbon cycle in the context of global climate change.

Through its potential to sequester or release large volumes of carbon, the boreal forest biome can exert significant impacts on the size of the atmospheric carbon pool and thus on the radiative properties of the atmosphere. Due to the large volume of carbon stored in its forest stands and largely frozen soils, this biome represents a particularly significant

\* Corresponding author. Code 923.4, NASA Goddard Space Flight Center, Greenbelt, MD 20771, USA. Tel.: +1-301-286-4862; fax: +1-301-286-0239.

E-mail address: [karl.huemmrich@gsfc.nasa.gov](mailto:karl.huemmrich@gsfc.nasa.gov) (K.F. Huemmrich).

global carbon pool, which may be disrupted in the face of increasing climate change. Northern latitude regions, including the boreal forest biome, are expected to undergo a disproportionate and rapid warming in response to global climate forcing (Houghton et al., 1996) that is predicted to enhance ecosystem carbon gain (photosynthetic) and carbon loss (respiratory) processes. Consequently, another objective of BOREAS was to explore controls on the boreal forest's carbon balance and to consider how this balance might change with current and expected future global warming.

BOREAS involved a major investment of funding and resources to acquire an extensive, diverse, and unique database of remote sensing imagery. Remote sensing science components of BOREAS were designed to develop and validate sensors, protocols, and algorithms for characterizing key biophysical properties of the boreal biome, with particular emphasis on those properties related to carbon and climate. Throughout BOREAS, remote sensing played a central role in the study, from the early planning phases, where it was employed during project design and field site selection, to the execution of intensive field campaigns (IFCs).

The scientific and logistical structure of BOREAS clearly resulted in a successful project: Approximately 500 scientific papers (not including this issue) have appeared to date, 123 in six BOREAS special issues (including three issues of *Journal of Geophysical Research—Atmospheres* [JGR], two issues of

*Tree Physiology*, and one issue of the *Canadian Journal of Remote Sensing* [CJRS]) (Hall, 2001). The importance of remote sensing science has been documented in a series of individual research papers in special issues of remote sensing journals (e.g., CJRS 1997) and remote sensing special sections of more general BOREAS special issues (e.g., JGR, 1997, 1999). However, a more broad synthesis of remote sensing science set in the context of overall BOREAS science objectives has yet to appear. Accordingly, the purpose of this article is to review remote sensing accomplishments from the perspective of the primary BOREAS science goals and to highlight key remote sensing contributions and shortcomings during several stages of the study. Based on progress to date, this review also offers recommendations for future remote sensing research.

## 2. BOREAS experimental design

The BOREAS study region encompassed a  $1000 \times 1000$ -km area spanning the north–south extent of the boreal biome from Manitoba to Saskatchewan in western Canada. Within this region were two smaller study areas—the northern study area (NSA) in Manitoba and the southern study area (SSA) in Saskatchewan. These were selected for intensive field measurements and located near the northern and southern boreal forest boundaries, respectively (Fig. 1).

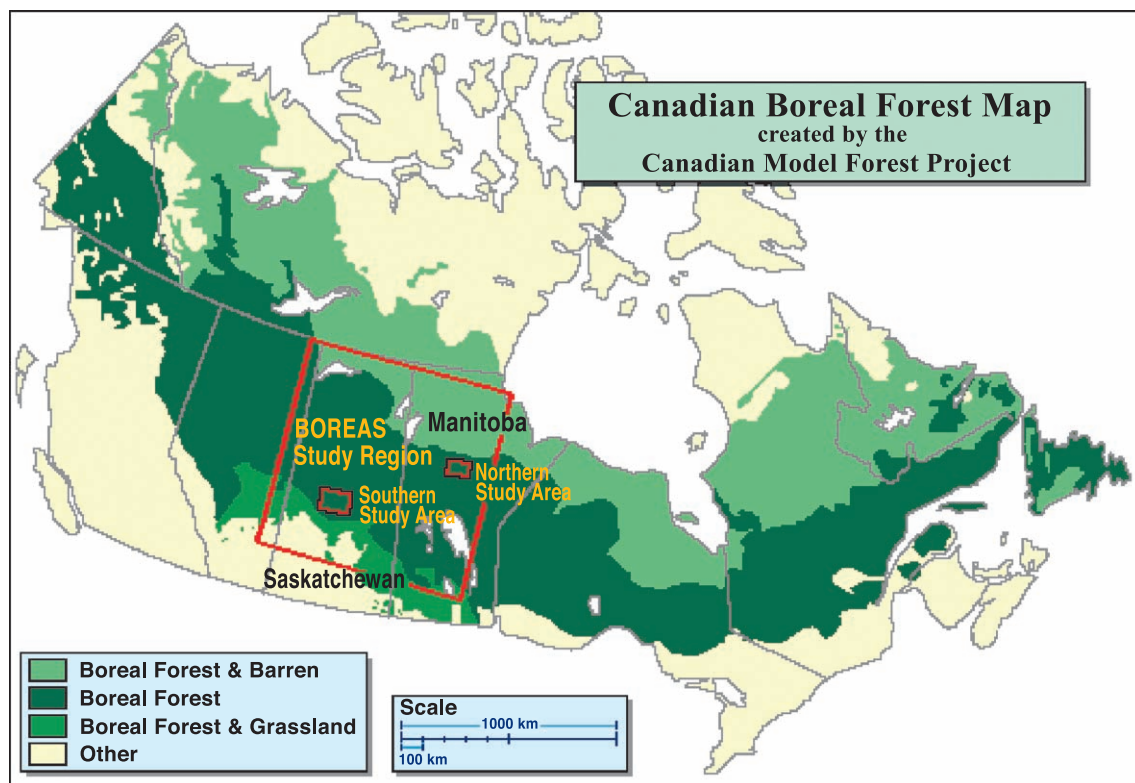


Fig. 1. Map of the Canadian boreal forest, showing the larger BOREAS study region (large rectangle) and two smaller study areas, the northern study area (NSA) and southern study area (SSA).

Additional sampling occurred along a defined transect between the two main study areas in the BOREAS region.

A formidable array of sensors and platforms was employed during BOREAS (Table 1), including satellite, aircraft, field, and laboratory sensors. Thus, a key aspect of BOREAS was its multi-scale design, enabling the evaluation of science questions at multiple spatial scales ranging from a single leaf to the entire boreal region.

Primary agencies leading BOREAS included the US National Aeronautics and Space Administration (NASA), the Canada Centre for Remote Sensing (CCRS), and the Natural Sciences and Engineering Research Council of Canada (NSERC), with considerable funding also provided by other sources, (see Acknowledgements). The study was divided into two phases: (1) the primary study phase, from 1993 to 1997, and (2) the secondary or “follow-on” phase, extending from 1997 to 2000. The primary study phase involved over 300 individuals divided into 85 science teams. The science teams were categorized by subject area: (1) Airborne flux and meteorology (AFM), (2) Tower Flux (TF), (3) Terrestrial Ecology (TE), (4) Trace Gas Biogeochemistry (TGB), (5) Snow and Hydrology (HYD), and (6)

Remote Sensing Science (RSS). BOREAS follow-on studies were limited to analysis of data previously collected during the primary (data collection) phase and included 26 science teams. During the primary study phase, there were 20 remote sensing science teams, whereas during the secondary phase, there were two remote sensing science teams. Additionally, BOREAS stimulated further follow-on activities, including the Canadian Boreal Ecosystem Research and Monitoring Sites (BERMS) program sponsored by the Meteorological Service of Canada (MSC), the Canadian Forest Service (CFS), and Parks Canada, with additional cooperation from the University of British Columbia and Queen’s University.

The unique combination of multidisciplinary science teams fostered a level of scientific integration rarely encountered during a single project. Activities were greatly facilitated by a science staff that assisted in the overall project coordination, field logistics, and data archiving, all of which were essential for the integrative aspects of the project (Newcomer et al., 2001). Large amounts of project data were archived at the Oak Ridge National Lab’s Distributive Active Archive Center (ORNL DAAC, accessible at <http://www->

Table 1  
Sensors, platforms, and measurements employed in BOREAS, along with selected publications describing these applications

Sensor	Platform	Measurements	References
Advanced Very High Resolution Radiometer (AVHRR)	satellite	multi-band spectral radiance, thermal emittance	Czajkowski et al., 1997
Landsat Thematic Mapper (TM)	satellite	multi-band spectral radiance, thermal emittance	Hall et al., 1997
SPOT	satellite	spectral radiance	Chen, Ju et al., 2003; Chen, Liu et al., 2003
GOES	satellite	spectral radiance (irradiance, PAR, and albedo)	Gu & Smith, 1997
ERS-1	satellite	radar backscatter	Way, Zimmermann, Rignot, McDonald, & Oren, 1997
NASA scatterometer (NSCAT)	satellite	radar backscatter	Frolking et al., 1999
SIR-C/XSAR	space shuttle	radar backscatter (C&L bands, polarimetric)	Saatchi & Moghaddam, 2000
AIRSAR	DC-8	radar backscatter (C, L&P bands, polarimetric)	Moghaddam et al., 2000; Saatchi & Moghaddam, 2000; Treuhart & Siqueira, 2000
Scanning Lidar Imager of Canopies by Echo Recovery (SLICER)	C-130	lidar tree heights and surface microtopography	Lefsky et al., 1999, 2002
Polarization and Directionality of Earth’s Radiation (POLDER)	helicopter and C-130	spectral radiance and BRDF	Bicheron et al., 1997
Advanced Solid-State Array Spectrometer (ASAS)	C-130	spectral radiance and BRDF	Russell et al., 1997; Sandmeier & Deering, 1999
Airborne Visible–Infrared Imaging Spectrometer (AVIRIS)	ER-2	hyperspectral radiance	Fuentes et al., 2001; Rahman et al., 2001
Compact Airborne Spectrographic Imager (CASI)	Piper Chieftan	spectral radiance	Hu et al., 2000; Zarco-Tejada & Miller, 1999; Zarco-Tejada et al., 2003
PARABOLA	suspended cables	BRDF	Li et al., 1997
Modular Multispectral Radiometer (Barnes)	helicopter	spectral radiance	Loechel et al., 1997
SE-590 (Spectron Engineering)	helicopter	spectral radiance	Nichol et al., 2000; Walthall, Williams, Dykes, & Young, 2001
Various portable spectroradiometers	ground-based (handheld or tripod)	spectral reflectance of canopy and stand elements	Middleton et al., 1997; Miller et al., 1997; Peddle, White, Soffer, Miller, & LeDrew, 2001

In many cases, spectral radiance is not measured directly but can be derived based on sensor calibration data.

[eosdis.ornl.gov/BOREAS/boreas\\_home\\_page.html](http://eosdis.ornl.gov/BOREAS/boreas_home_page.html)) for continuous open distribution and ongoing analysis. In addition, a CD-ROM (Compact Disk–Read Only Memory) set containing key BOREAS data sets is also available through the ORNL DAAC (Newcomer et al., 2001).

BOREAS remains a “work in progress.” While BOREAS as a formal NASA program has ended, the data analysis and synthesis continues, new publications continue to emerge, and knowledge of the boreal ecosystem continues to expand. One of the legacies of the BOREAS project will undoubtedly be its extensive collection of remote sensing data sets. Accordingly, this paper is intended both to synthesize remote sensing science progress to date and to provide a context for future analysis of what is likely one of the largest and most comprehensive remote sensing data sets acquired in conjunction with extensive ground validation over any region to date.

### 3. Early remote sensing results

During the early stages of BOREAS, a number of key remote sensing products emerged, including regional maps of vegetation cover types and biophysical parameters. One realization from these early maps was that a significant portion of the BOREAS region, covering approximately 23–30% of the study area, had been disturbed by recent fires and logging (Hall, Knapp, & Huemmrich, 1997; Steyaert, Hall, & Loveland, 1997). These early studies also revealed key differences in the functional and reflectance properties of its dominant vegetation types (Fig. 2). Aspen, black spruce, jack pine, and fen are strikingly different in their physiological and hydrological properties and thus exhibit contrasting degrees of control on the ecosystem–atmosphere exchanges of carbon dioxide, water vapor, and sensible heat (Baldocchi, Kelliher, Black, & Jarvis, 2000). Fens, which cover approximately 7% of the region (Hall et al., 1997), emerged as significant contributors to regional methane emissions (Moosavi & Crill, 1997). However, these key cover types were not fully distinguishable by early Landsat Thematic Mapper (TM) and Advanced Very High Resolution Radiometer (AVHRR) based land-cover products (Hall et al., 1997), thus leading to questions regarding the capability of remote sensing science to provide the land-cover products needed to correctly represent ecosystem function and surface-atmosphere transport processes. This challenge spawned the development of a variety of new remote sensing algorithms for land-cover classification and biophysical parameter estimation, as presented in Section 4 of this paper.

Another significant early finding from remote sensing analyses was that many ecosystem model assumptions regarding canopy structure for this biome were not well founded. The common assumption of a horizontally homogeneous canopy medium used by many models and the parameterization of the canopy as a single vertical layer

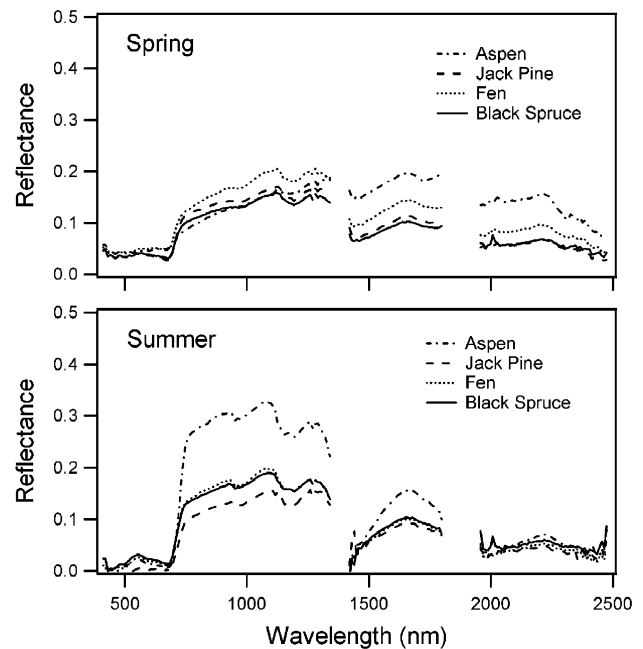


Fig. 2. Representative reflectance spectra for four of the seven dominant boreal cover types in early spring before substantial leaf-out (April 1994) and in midsummer (July 1994). Note low overall reflectance (albedo), particularly for conifers (jack pine and black spruce). Additional major cover types (not shown) include water, mixed (conifer and deciduous), and recently disturbed stands. Each spectrum is a mean of 100 pixels collected from BOREAS flux tower sites with the AVIRIS sensor. Blank spectral regions indicate wavelengths of insufficient signal due to strong atmospheric water absorption. For further description of sites and AVIRIS processing procedures, see Fuentes et al. (2001).

emerged as especially inappropriate, particularly at horizontal scales between a few meters and 1 km. The often sparse and clumped spruce and jack pine stands, typically underlain by a surface layer of moss or lichens, were the most notable examples. Remote sensing products from early in the study—many derived using large pixels, from a small number of broad spectral bands, and an assumption of stand homogeneity—were ill-suited to characterize the complex vertical and horizontal distributions of vegetation structural elements of this biome (Walthall et al., 1997). Because the net gas exchange of this biome appeared to be primarily influenced by light absorption and other physical processes (Goulden et al., 1997), and because of the strong influence of stand structure on the surface radiation budget, improved characterization of the three-dimensional vegetation structure emerged as a critical need. Priority concerns that received much attention by remote sensing teams during the later stages of BOREAS were the characterization of canopy clumping, the bidirectional reflectance distribution function (BRDF), leaf area index (LAI), and the two-layered structure of many boreal forest stands. The emergence of these issues in the early stages of BOREAS led to improved remote sensing methods and products.



Perhaps the single most significant discovery during these early stages of BOREAS was that the surface albedo used for the boreal biome in regional numerical weather prediction models was grossly inaccurate. Remote sensing measurements confirmed early observations (Betts & Ball, 1997) that this biome (especially its coniferous stands) was substantially darker than had previously been assumed (Fig. 2). This is particularly the case for the winter period when exposed snow-free forest canopies exhibit significantly lower albedos (typically 0.2–0.3) than the higher values (0.6–0.8) previously assumed in operational weather models (Gu & Smith, *this issue*). Low albedos have important implications for any type of environmental model seeking to simulate the surface-atmosphere exchanges of mass and energy. Consequently, in the later stages of BOREAS, much effort was directed towards a detailed assessment of surface reflectance patterns. Significant improvements in numerical weather prediction models and regional weather forecasts resulted from the inclusion of more realistic surface albedos for boreal forests derived from the BOREAS observation program; see Betts, Viterbo, Beljaars, and van den Hurk (2001), Sellers et al. (1997), and Viterbo and Betts (1999). This revision explained why these models had consistently underestimated boreal winter air temperatures by as much as 15 °C (Sellers et al., 1997). The findings concerning boreal forest albedos illustrated the advantages of using direct measurements and the perils of relying on past literature values for modeling experiments.

These advances highlighted the need for improved remote sensing-based land-cover products that adequately define surface heterogeneity for improved extrapolation and characterization of regional processes. For example, tower flux (eddy covariance) measurements and other detailed biophysical studies from BOREAS revealed marked differences in carbon uptake, storage, and release among needle-leaf evergreen and broad-leaf deciduous forests, bogs, fens, and other wetland features, yet some of these land-cover categories become confounded in many remote sensing products at spatial scales greater than approximately 1 km. Subsequent SVAT (Soil–Vegetation–Atmosphere Transfer) modeling studies revealed that adequate representation of sub-grid-scale heterogeneity in land cover, particularly between deciduous and coniferous growth forms and wetlands, is critical for accurate regional extrapolations of stand level carbon exchange dynamics (e.g., Kimball, Running, & Saatchi, 1999; Potter, Coughlin, & Brooks, 1999). Thus, improved definition of surface properties became key remote sensing goals in BOREAS.

#### 4. Remote sensing in BOREAS

The remote sensing science of BOREAS has improved our understanding of the boreal forest in four principal areas: (1) definition of vegetation structure, (2) land-cover classification, (3) assessment of the carbon balance, and (4)

links between surface properties, weather, and climate. These four areas are highlighted below.

##### 4.1. Improved definition of vegetation structure

Responding to the need for more realistic definition of vegetation structure and light absorption, several BOREAS science teams developed novel methods of describing vegetation structure. Most of these methods employed optical sensors of vegetation properties or radiative transfer models that can be readily linked to airborne or satellite remote sensing products. These methods offer a range of new tools for field validation of key biophysical parameters derived from remote sensing, as well as insights into parameterizations needed for canopy models appropriate to the boreal landscape.

Significant improvements in our understanding of canopy structure were gained by assessment of vegetation “clumping” at several scales, ranging from a single branch tip to an entire stand. Many of these studies were directed at defining and estimating leaf area index (LAI), a metric of foliage density that has been shown to exert a strong influence on the biosphere–atmosphere exchange of energy, water, and carbon (Running & Coughlan, 1988). LAI is traditionally defined as the total one-sided leaf area divided by the subtending ground area (Nobel & Long, 1985), largely based on broad-leaf crop studies. Unfortunately, this definition is of little practical or theoretical use for much of the world’s vegetation. For the needle-leaved and moss-covered boreal forest, it remains a difficult challenge to establish a meaningful operational concept of LAI and to relate this to the effective LAI, e.g., the functional leaf area estimated from radiation interception. Consequently, a number of BOREAS teams addressed the need for improved definition and characterization of LAI, and modified versions of the traditional LAI definition were often adopted (e.g., Chen, Rich, Gower, Norman, & Plummer, 1997).

At the branch tip scale, Serrano, Gamon, and Berry (1997) developed an innovative method of assessing leaf area index using an integrating sphere. This method compared well with conventional methods (e.g., Johnson, 1984; Nobel & Long, 1985) and provided a rapid method for assessing “effective” leaf area for light absorption on intact shoots. This method is particularly convenient for plants with small or needle-shaped leaves (e.g., conifers).

At the level of the intact stand, Chen and Cihlar (1995) developed a novel optical method of assessing effective LAI and foliage clumping using a mobile PAR sensor along transects below the forest canopy (the Tracing Radiation and Architecture of Canopies [TRAC] instrument). One practical benefit of this method is that it measures the intact forest, incorporating vegetation clumping at the branch, canopy, and stand scales. The resulting “clumping index” provides one way to relate the fraction of photosynthetically active radiation absorbed ( $F_{\text{PAR}}$ ) or the effective (optical absorb-

ing) LAI of the entire stand to the leaf area index traditionally measured by destructive harvests (Chen, Rich et al., 1997). Another novel optical approach for measuring canopy LAI and structure used in BOREAS was the multiband vegetation imager (MVI) (Kucharik, Norman, Murdock, & Gower, 1997). The MVI viewed the canopy from below and captured images in both visible and near infrared bands. The use of two bands permitted identification of sunlit and shaded foliage, sunlit and shaded branches, clear sky and clouds. MVI data input in to a Monte Carlo canopy simulation model were used to determine LAI, clumping factors, leaf angle distribution, and branch area for BOREAS sites (Kucharik, Norman, & Gower, 1998a, 1998b, 1999). Together, these optical methods of assessing overstory foliage structure offer practical alternatives to the more traditional definition of LAI based on destructive harvests and are likely to influence future vegetation studies requiring characterization of stand structure.

A key feature of boreal stand structure is the horizontal variability in density. Examining the effects of spatial scale on the estimation of LAI, Fernandes et al. (this issue) estimated LAI at a fine (less than 30-m) scale using the FLIM-CLUS algorithm and compared this estimate with LAI estimated at coarser (up to 1-km) scales. At coarse scales, sub-pixel-sized open areas had a measurable effect on the determination of LAI. This illustration of the scale dependence of LAI estimates has implications for the field verification of coarse-scale LAI, since ground validation is often weighted towards forested stands, with cleared areas being ignored or under-sampled.

A fundamental challenge to the retrieval of useful land-cover and biophysical products (e.g., LAI) from remote sensing is the complex stand structure, particularly the two-layered canopy (e.g., conifer forests on top of a surface moss or lichen layer), and the varying degree of canopy closure. When combined with changing sun angles, these structural complexities yield spatially and temporally variable reflectance patterns that often confound the estimation of cover type or biophysical parameters from remote sensing. For example, the variation in the optical signatures of the open boreal forests are largely due to variability in the understory, rendering standard, index-based approaches to generating forest LAI questionable (Chen & Cihlar, 1996; Chen, Leblanc, Cihlar, Desjardins, & MacPherson, 1999; Hu, Inannen, & Miller, 2000). Using airborne Compact Airborne Spectrographic Imager (CASI) data from two seasons, Hu et al. (2000) took advantage of winter snow cover information to isolate overstory from understory and yield more accurate retrieval of overstory LAI and canopy closure. Further, Hu, Miller, Chen, and Hollinger (this issue) determined LAI for several sites using principal components analysis to define spectral endmembers coupled with a linear mixture model to determine the proportion of each endmember in a pixel. Wintertime CASI data were used where the background was snow covered, minimizing the effect of understory reflectance variation. These methods demonstrated how multi-

temporal sampling could be used to evaluate the effect of individual forest layers on the overall stand signals. Further work has revealed that moss cover may account for 60% of the BOREAS landscape (Rapalee, Steyaert, & Hall, 2001). Given this large spatial extent of moss cover in the boreal biome, the gradient of stand densities, including significant areas of sparse forest towards the northern boreal–tundra transition zone, and the large impact of understory vegetation on surface properties and biosphere–atmosphere exchange, further characterization of this understory component in the boreal biome is warranted, as recommended by Miller et al. (1997).

Our understanding of forest stand structure benefited greatly from multiangle instruments, including the POLDER (Polarization and Directionality of Earth Reflectance) sensor (Deschamps et al., 1994). A primary goal for this sensor was to characterize the vegetation Bidirectional Reflectance Distribution Function (BRDF) and define the “hot spot” (i.e., the reflectance bright spot that occurs when the view angle approaches that of the solar beam). Studies with POLDER revealed that the hot spot did not appear as angularly narrow as predicted by radiation transfer models (Bréon et al., 1997), laying the foundation for improvements in these models. Furthermore, model inversion of multi-scale POLDER hot spot signatures provided key architectural parameters (Lacaze & Roujean, 2001). For example, the clumping of forest stands (Lacaze, Chen, Roujean, & Leblanc, 2002) can be assessed in this way, providing a powerful method for yielding both effective and traditional LAI maps of the boreal biome. The spatial distribution of architectural parameters can also be applied to functional vegetation mapping, as described below (see Section 4.2).

BOREAS studies have shown radar interferometry to be a promising tool for deriving forest stand structure through the use of the Topographic Synthetic Aperture Radar (TOPSAR) instrument of NASA Jet Propulsion Laboratory’s (JPL) airborne Synthetic Aperture Radar (AIRSAR). At the time of the BOREAS AIRSAR data acquisitions, the estimation of canopy height and characterization of vertical stand structure had not yet been demonstrated, and data requirements were not fully known. Therefore, the data acquisition scenario was not optimized, limiting the successful application of radar during BOREAS. Nevertheless, TOPSAR was used to obtain canopy height estimates (Treuhart & Siqueira, 2000). These initial TOPSAR studies established a framework for more detailed characterization of stand-level structure through interferometric SAR (INSAR) data with multiple baselines. In subsequent studies, multiple baseline INSAR data, obtained by sampling at multiple altitudes, enabled the characterization of canopy vertical profiles and were used to derive leaf area density profiles in conjunction with hyperspectral optical data (Treuhart, Asner, Law, & vanTuyl, 2002).

A number of radiative transfer models have been developed that provide more realistic assessment of three-dimen-

sional canopy structure for the boreal forest. BOREAS data sets have been instrumental to the validation and further application of several models, including DART (Gastellu-Etchegorry et al., 1999), 4-Scale and 5-Scale (Chen & LeBlanc, 1997, 2001; Leblanc & Chen, 2000), FLAIR (White, Miller, & Chen, 2001, 2002), FLIM (Rosema, Verhoef, Noorbergen, & Borgesius, 1992) and FLIM-CLUS (Fernandes, Hu, Miller, & Rubinstein, 2002; Hu et al., 2000), GeoSail (Huemmrich, 2001), GHOST (Lacaze & Roujean, 2001), GOMS (Li & Strahler, 1992) and GORT (Li, Strahler, & Woodcock, 1995), and various Monte Carlo models, including SPRINT (Goel & Thompson, 2000; North, 1996). Many of these models have improved the characterization of boreal vegetation, biophysical parameters, and surface properties by accounting for vegetation canopy or stand structure. Because these models characterize vegetation according to physical principles rather than by statistical correlations, they can often provide more realistic or robust assessments of biophysical parameters, potentially reducing the need for empirical calibrations (Hall et al., 1997). For example, using a physically based approach to integrated land-cover classification and biophysical parameter estimation, Hall et al. (1997) mapped biomass density in the BOREAS SSA with a standard error of  $2.73 \text{ kg m}^{-2}$ . Furthermore, with the introduction of a needle-scale model (LIBERTY, Dawson, Curran, & Plummer, 1998), simulations with coupled leaf and canopy models have begun to provide new insight into the factors affecting biophysical parameter retrieval in boreal conifer forests (Dawson, Curran, & North, 1999). Zarco-Tejada et al. (2003) estimated needle chlorophyll content using a model inversion approach applied to 72-band CASI data. In that study, the SPRINT canopy reflectance model (Goel & Thompson, 2000) was coupled with the PROSPECT leaf optical property model (Jacquemond & Baret, 1990) to successfully determine jack pine needle chlorophyll content. In another example, the 5-Scale model (Leblanc & Chen, 2000), merging the LIBERTY and 4-Scale models, has been used successfully for large area land-cover classification. This approach was extended by Peddle, Johnson, Cihlar, and Latifovic (2003) by using the 5-Scale model to obtain LAI estimates within  $\pm 0.5$ , validated at over 60 plots in the SSA, transect, and NSA, together with detailed land-cover information (discussed in next section).

#### 4.2. Improved land-cover classification

Land cover was one of the most fundamental and important information requirements of BOREAS remote sensing, serving a wide variety of purposes amongst many BOREAS science teams and projects (Hall, 1999; Potter et al., 1999; Sellers et al., 1997). A summary of land-cover classification results, representing most of the boreal land-cover products published in BOREAS Special Issues and BOREAS data reports to date, is contained in Table 2. Even though land-cover classification has a long history in remote

sensing science (Cihlar, 2000; Steyaert et al., 1997), significant improvements were made during BOREAS through the use of new classification approaches, new sensors, and novel sensor combinations. A full description of these boreal land-cover products is beyond the scope of this review. Instead, selected examples are briefly presented here.

A set of 13 land-cover classes (Table 3) was identified for BOREAS modeling and other purposes at a joint meeting of the Terrestrial Ecosystem (TE) modelers and the Remote Sensing Science (RSS) algorithm developers in Columbia, MD, in June 1993 (Sellers et al., 1994, 1995) and subsequently endorsed by AFM, TF, and TGB science team modeling groups. This TE/RSS class set, or subsets thereof, was used in a majority of the BOREAS land-cover classifications shown in Table 2, particularly at the spatial resolution of Landsat imagery (30 m). Alternative class structures (e.g., Table 4) derived from the International Geosphere Biosphere Project (IGBP, see Belward, 1996) were used primarily with regional-scale studies using coarser spatial resolution AVHRR imagery and, more recently, with Landsat image mosaics. In some cases, these were associated with larger national-scale mapping projects (e.g., Cihlar, Chen et al., 2002; Cihlar, Guindon et al., in press).

Early in BOREAS, Hall and Knapp (1994) used Landsat imagery and a standard supervised maximum likelihood (ML) approach to provide initial land-cover products for 11 of the 13 TE/RSS classes covering the full SSA and NSA ( $129 \times 86 \text{ km} = 11,094 \text{ km}^2$  each). These products had an average accuracy of 70% ( $k=0.60$ ) based on evaluations of five classes (classes 1–5, Table 3) for which field validation data existed (Hall & Knapp, 1994). Additional validation sites were identified in the SSA during the 1994 IFCs and incorporated into a revised validation released in 1995 (Hall & Knapp, 1999a) that showed a higher accuracy for these five classes (78%).

A physically based classification (PBC) approach was introduced by Hall and Knapp (1996, 1999b) and Hall et al. (1997) using canopy geometric optical reflectance model output to describe the spectral reflectance of different land-cover types, identified as different trajectories in spectral space. These models provide an explicit linkage between three-dimensional forest structure and satellite image spectral reflectance to yield not only land cover but also fully integrated biophysical information (e.g., biomass, LAI, stand attributes). Physically based modeling does not require training data, avoids the restrictive statistical assumptions of conventional classifiers that are often violated, and provides an explicit mechanism to account for interannual and multi-scene reflectance variation caused by changes in solar position, viewing angle, topography, and other factors. Compared to the initial ML classifications of Hall and Knapp (1994, 1999a), the physically based Landsat products yielded higher accuracies over a larger number of classes. The NSA PBC classification accuracy was 85%



Table 2

Summary of BOREAS land-cover classification products published in BOREAS Special Issues and BOREAS data reports

Reference [BOREAS Team]	Sensor	Algorithm	Classes	Area	Image date(s)	Number Classes	Accuracy % (Kappa)	Validation source	Comments
Hall & Knapp, 1994 [TE-18]	Landsat-5 TM (30 m) Bands 1–5,7	maximum likelihood	TE/RSS classes	SSA:NSA: 10 <sup>4</sup> km <sup>2</sup> each	August 6, 1990; August 20, 1988	11 (8 forest); 11 (8 forest)	67% (0.56); 73% (0.63) [five classes each]	<27 sites 37 sites, <i>n</i> = 333 TF/Aux Sites, 3 × 3 pixels/site	initial product
Hall & Knapp, 1999a [TE-18]	Landsat-5 TM (30 m) Bands 1–5,7	maximum likelihood	TE/RSS classes	SSA: 10 <sup>4</sup> km <sup>2</sup>	August 6, 1990	11 (8 forest)	78% (0.66) [five classes]	27 sites, <i>n</i> = 243 TF/Aux Sites, 3 × 3 pixels/site	updated validation of initial product
Hall & Knapp, 1996; Hall et al., 1997 [TE-18]	Landsat-5 TM (30 m) Bands 3,4,5 reflectance	physically based canopy modeling	TE/RSS classes	SSA: 10 <sup>4</sup> km <sup>2</sup>	September 2, 1994	13 (9 forest)	70% (0.59) [nine classes]	35 sites, <i>n</i> = 315 TF/aux sites, field 3 × 3 pixels/site	includes biophysical parameters; initial product
Hall & Knapp, 1999b [TE-18]	Landsat-5 TM (30 m) Bands 3,4,5 reflectance	physically based canopy modeling	TE/RSS classes	SSA:NSA: 10 <sup>4</sup> km <sup>2</sup> each	September 2, 1994; June 21, 1995	13 (9 forest); 11 (8 forest)	75% (0.70); 85% (0.83)	48 sites, <i>n</i> = 432, 68 sites, <i>n</i> = 612 TF/aux sites, field sites 3 × 3 pixels/site	update SSA new NSA includes biophysical parameters
Peddle, 1999; Peddle et al., 1997 [TE-18, RSS-19]	Landsat-5 TM (30 m) Bands 3,4 reflectance	GOMS physical canopy model and evidential reasoning	TE/RSS classes	SSA	September 2, 1994	13 (9 forest)	85% (0.83)	40 sites, <i>n</i> = 992, TF/aux sites, field sites 5 × 5 pixels/site	also has biophysical parameters
Steyaert et al., 1997 [AFM-12, TE-18]	NOAA-11 AVHRR NDVI composites (1 km)	unsup. clustering; field labels	TE/RSS classes	region 5 × 10 <sup>5</sup> km <sup>2</sup>	April–September 1992	16 (9 forest)	class areas: (relative comparison—no %, K)	agreement with <a href="#">Hall and Knapp (1994)</a> TM products (SSA, NSA)	also mapped forest fires
Cihlar et al., 1997 [TE-16]	NOAA-11 AVHRR composites (1 km)	ECM and CPG	IGBP	full region 10 <sup>6</sup> km <sup>2</sup>	April–October 1993	32; grouped to 5 (4 forest)	57% (0.30) [all] to 89% (0.78) [pure pixels only]	agreement with <a href="#">Hall and Knapp (1994)</a> TM products (SSA, NSA)	Canada-wide land cover, biophysical products
Ranson et al., 1997 [RSS-15]	SIR-C/XSAR & Landsat TM	maximum likelihood and PCA	forest species/ nonforest	SSA (~MSA) 3 × 10 <sup>3</sup> km <sup>2</sup>	1994—Radar: April 15/October 6; TM: September 2	7 (3 forest)	87.3%	62 field plots	also has biophysical information (separate)
Beaubien et al., 1999, 2000 [TE-16]	7 scene mosaic Landsat-5 TM Bands 3,4,5	ECM	IGBP/GOFC	SSA, NSA, transect 10 <sup>5</sup> km <sup>2</sup>	June–August 1991–1998	28 (17 forest)	91% (0.89)	TF/aux sites, field sites <i>n</i> = 238	
Peddle et al. (2003)	7 scene mosaic Landsat-5; Bands 3,4	MFM-5-Scale canopy model	IGBP/GOFC	SSA, NSA, and transect	June–August. 1991–1998	13 forest: 25 classes (17 forest)	85% (0.83); 80% (0.78)	136 field sites; agreement with <a href="#">Beaubien et al., 2000 (<i>n</i> = 11,442)</a>	also has biophysical parameters
Zarco-Tejada & Miller, 1999 [RSS-19]	CASI 16 bands 3-m reflectance	red-edge	subset of TE/RSS classes	SSA (~MSA) 192 km <sup>2</sup>	August 1, 1996	7 (4 forest)	61% (0.52)	agreement with SERM map (MSA) <i>n</i> = 2646	foliar chemistry parameters possible
Fuentes et al., 2001	AVIRIS 20 m 53 bands (of 224 bands) used	spectral mixture analysis & maximum likelihood	subset of TE/RSS classes	SSA (~MSA) 120 km <sup>2</sup>	April 19, 1994, July 21, 1994, and September 16, 1994	7 (4 forest)	80% (0.77)	agreement with SERM map (MSA) <i>n</i> = 700	water and foliar chemistry parameters possible

Other studies discussed in this paper are also included. Validation sites listed include tower flux (TF) and auxiliary (AUX) field sites.

Table 3  
BOREAS TE/RSS land-cover classes

Class	Description
1	conifer (wet)
2	conifer (dry)
3	mixed (coniferous and deciduous)
4	deciduous
5	fen
6	water
7	disturbed
8	fire blackened
9	new regeneration conifer
10	medium-age regeneration conifer
11	new regeneration deciduous
12	medium-age regeneration—deciduous
13	grass

for 11 classes (Hall & Knapp, 1999b). The SSA was initially classified using PBC with an accuracy of 70% for 9 classes (Hall & Knapp, 1996; Hall et al., 1997) over a larger area ( $144 \times 114 \text{ km} = 16,416 \text{ km}^2$ ), with a subsequent and more extensive validation for all 13 classes yielding an accuracy of 75% for the same area (Hall & Knapp, 1999b). This was further improved to 85% by Peddle, Hall, LeDrew, and Knapp (1997), using a more advanced canopy model (GOMS: Li & Strahler, 1992; Peddle, Hall, & LeDrew, 1999) coupled with an evidential reasoning image classifier (Peddle, 1995, 1999).

The entire BOREAS region ( $1000 \times 1000 \text{ km}$ ) was initially classified using NOAA AVHRR imagery and various unsupervised classification approaches. Steyaert et al. (1997) mapped over half of the BOREAS region ( $821 \times 619 \text{ km} = 508,199 \text{ km}^2$ , encompassing the full SSA and NSA) from NDVI composites throughout the 1992 growing season using a conventional clustering algorithm and field-based cluster labeling to achieve a 16-class final product, as well as forest fire and regeneration maps. Cihlar, Beaubien, Xiao, and Li (1997) mapped the entire BOREAS region as part of a larger, Canada-wide set of land-cover and biophysical products based on 1993 AVHRR composites. Using Classification by Progressive Generalization (CPG, Cihlar, Xiao, Beaubien, Fung, & Latifovic, 1998) and the Enhancement-Classification Method (ECM, Beaubien, Cihlar, Simard, & Latifovic, 1999), 32 IGBP classes were identified throughout the boreal zone. ECM involves subjective user interaction to maximize image information from classification based on image contrast enhancement, quantization, filtering, clustering, minimum distance reclassification, and cluster grouping and labeling. CPG reduces the potential for bias in the cluster groupings step by progressively generalizing clusters based on spectral and spatial proximity measures to match the desired number of classes. Accuracy was assessed as agreement with 5 of the 11 classes from the Hall and Knapp (1994) initial ML products in the SSA and NSA. AVHRR pixels often contained multiple land-cover classes, thus affecting results obtained. ECM and CPG results were similar, and ranged from 57% (all pixels)

to 89% (subsample of pure AVHRR pixels) for these five classes.

A mosaic of seven Landsat TM images covering the entire BOREAS region was classified by Beaubien et al. (1999) and Beaubien, Latifovic, Cihlar, and Simard (2000) using a modified ECM approach to produce 28 detailed forest land-cover classes adhering to IGBP/GOFC standards (Table 4). An overall accuracy of 91% was obtained (Beaubien et al., 2000) from validation against a large sample of tower flux, auxiliary and additional ground-verified sites throughout the BOREAS SSA, transect, and NSA. However, ECM is rather subjective and labor intensive, and it does not provide biophysical parameter estimates. These issues were addressed by Peddle et al. (2003) using the Multiple-Forward-Mode (MFM) modeling approach (Peddle, Franklin, Johnson, Lavigne, & Wulder, in press), coupled with the 5-Scale model of Leblanc and Chen (2000). MFM-5-Scale was applied to the same seven-image Landsat mosaic (Beaubien et al., 2000) for 25 IGBP/GOFC classes (the high-, medium-, and low-density crop classes were combined into one crop class; cloud class excluded). A set of 13 detailed forest classes was classified with an accuracy of 85% validated against independent field data from Beaubien et al. (2000), with good accuracy indicated (80%) for all 25 classes based on agreement with the ECM map from Beaubien et al. (2000) over a large sample. MFM-5-Scale has also been used to label unsupervised clusters generated by CPG (Cihlar et al., 1998; Peddle, Johnson, Cihlar, Leblanc, & Chen, in press). An important advantage

Table 4  
IGBP/GOFC classes used in regional-scale land-cover classifications

Class	Description	Class	Description
1	conifer, high density: BS	15	mixed deciduous (>60%)
2	conifer, high density: BS/JP	16	mixed forest
3	conifer, high density: YBS	17	wetland, shrubs, grasses
4	conifer, medium density: JP	18	burn—recent; bare area
5	conifer, medium density: BS/JP	19	burn—recent; sparse vegetation
6	conifer, medium density: BS	20	burn; rock outcrops
7	conifer, low density: BS/JP	21	older burns, shrub—grass cover
8	conifer, low density: JP	22	old burns, mixed regeneration cover
9	conifer, very low density	23	bare, disturbed areas
10	deciduous, high density	24	crop—high biomass
11	deciduous, medium density	25	crop—medium biomass
12	deciduous, low broadleaf cover	26	crop—low biomass
13	mixed conifer (>60%) high density	27	water
14	mixed conifer (>60%) medium density	28	clouds

Conifer and deciduous classes [1–12] were >80% abundance, with crown densities quantified as high (>60%), medium (40–60%), low (25–40%), and very low (<25%). Species legend: Black Spruce (BS), Jack Pine (JP); (Y prefix = young).

of the independent MFM-5-Scale approach is its provision of biophysical information (Section 4.1, above) and a more objective, semiautomated approach that is appropriate for broader applications (e.g., regional/national scales, multi-temporal studies, etc.) with the potential to provide an integrated, operational process.

Fernandes et al. (2003) examined several algorithms for mapping sub-pixel land-cover fractions and continuous fields of vegetation properties in the BOREAS study area. They used Landsat TM-based land-cover classification scaled up to the 1.15-km pixel size of SPOT VEGETATION imagery. The neural network, look-up-table, and multivariate regression algorithms performed well when the training and validation regions were in close proximity; however, when these regions were more distant, all three methods exhibited substantial biases owing to characteristics of the training data. Linear least-squares inversion showed less bias, but was also less precise. A combination of multivariate regression and linear least-squares inversion was recommended for the general case, for which woody fraction estimates were within 20% of those obtained from Landsat TM classification.

Airborne hyperspectral sensors such as the Compact Airborne Spectrographic Imager (CASI) and the Airborne Visible/Infrared Imaging Spectrometer (AVIRIS) offer greater spectral detail than multi-band sensors (Table 1) and have the potential to provide finer definition of vegetation types and functional states than previous maps based on AVHRR or TM. Using the CASI sensor, Zarco-Tejada and Miller (1999) demonstrated that four statistics defining the shape and position of the reflectance spectrum near 700 nm (i.e., “red-edge” parameters) can lead to improved vegetation mapping (61% for seven of the TE/RSS classes) for a small portion (192 km<sup>2</sup>) of the SSA, relative to the accuracy estimated within the corresponding area extracted from an earlier Landsat classification (Hall et al., 1997). Optical parameters characterizing the red edge are known to be responsive to variations in leaf pigment content, LAI, and understory. The fen, in particular, which was not easily resolved by several other sensors, was readily distinguished with these red-edge parameters. However, for a single date, the red-edge parameters were unable to clearly distinguish wet from dry conifers (e.g., black spruce vs. jack pine), two functionally distinct vegetation classes that differ little in this spectral region. Using AVIRIS imagery, Fuentes, Gamon, Qiu, Sims, and Roberts (2001) classified TE/RSS classes 1–7 (Table 3) with an accuracy of 80% over a small (120 km<sup>2</sup>) area. This study tested two separate approaches to utilizing the fine-spectral resolution present in AVIRIS imagery. One method used several reflectance indices known from prior field and experimental studies to have specific physiological or structural significance. These indices included narrow-band formulations of the normalized difference vegetation index (NDVI, an indicator of green canopy structure), the photochemical reflectance index (PRI, an indicator of chlorophyll and carotenoid pigment

levels, including xanthophylls cycle pigments), and the 970-nm water band index (WBI, an indicator of canopy water content). Index maps derived from reflectance were then used in a supervised maximum likelihood classification to map the local region around several SSA tower sites. A second method used a library of leaf spectral signatures representing contrasting levels of the major visible leaf pigment groups (chlorophylls, carotenoids, and anthocyanins) for spectral mixture analysis. The resulting end-member fraction maps illustrating relative amounts of hypothetical “leaf types” (based on these *in vivo* pigment reflectance spectra) were then used in a supervised classification routine to map the same SSA tower site regions, yielding a classification accuracy of 80.1% (Fig. 3). More recent work employing supervised classification on multiple narrow bands have reported improved accuracies of up to 91% (Fig. 3, Fuentes et al., unpublished).

A general problem in remote sensing is that it is often difficult to compare different land-cover products due to the multiple sensors, algorithms, landscapes, image dates, cover classes, and accuracy assessment methods used. Because of these multiple variables, a direct comparison of the reported accuracies of all land-cover products (Table 2) is usually not particularly meaningful. An objective and comprehensive comparison would require a more rigorous experimental

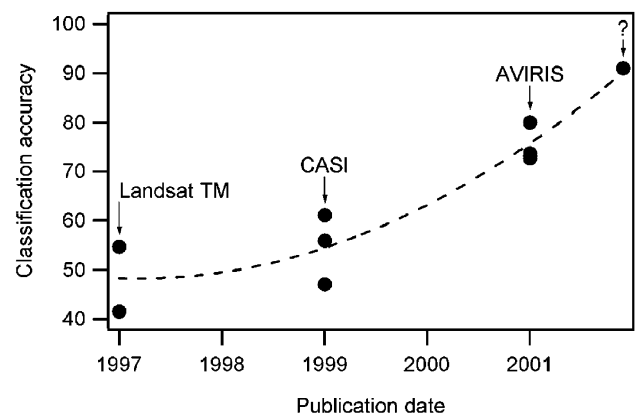


Fig. 3. Overall classification accuracy for various land-cover products obtained for a small BOREAS subregion (Jack Pine-Fen in the SSA). Land-cover products were derived from Landsat TM (Hall et al., 1997), CASI (Zarco-Tejada & Miller, 1999), AVIRIS (Fuentes et al., 2001), and more recent unpublished AVIRIS results (question mark—Fuentes, personal communication). The Landsat TM land-cover result was extracted from a much larger map (full SSA) with a reported overall accuracy of 75% (Hall & Knapp, 1999a, 1999b; Hall et al., 1997; see Table 2). For this figure, comparable accuracy assessment methods were applied to all products using a common “ground truth” from the SERM map as described in Fuentes et al. (2001) and Zarco-Tejada and Miller (1999). For Landsat TM, the two different points represent the accuracies reported in Fuentes et al. and Zarco-Tejada and Miller over the smaller modeling sub-area (covering ~1% of the SSA). For CASI, the multiple data points indicate different methods of land-cover retrieval. For AVIRIS, the multiple data points indicate both different retrieval methods and overpass dates. See Fuentes et al. and Zarco-Tejada and Miller for further discussion of methods and accuracy assessment.



design than was possible in BOREAS. However, because of the abundance of land-cover products over the same region, and because of the provision of common sources of “ground truth,” BOREAS provided an opportunity to explore relative accuracies of several different approaches in a more objective way than is usually the case. The results of an initial comparison of three land-cover products are shown in Fig. 3, which reports the overall accuracies for 7 classes from the 13-class TE/RSS class set for a relatively small area ( $\sim 1\%$  of the SSA) using land-cover products from three sensors: Landsat TM (Hall et al., 1997), CASI (Zarco-Tejada & Miller, 1999), and AVIRIS (Fuentes et al., 2001). In this analysis, comparable accuracy assessment methods (reported in Fuentes et al., 2001; Zarco-Tejada & Miller, 1999, and differing from those reported in Hall et al., 1997), a common “truth”—the Saskatchewan Environment and Resource Management (SERM) land-cover map, and the same seven classes (see Fig. 4 and Table 3) were applied to a single boreal landscape (the Fen–Jack Pine subregion within the SSA, a portion of which is illustrated in Fig. 4). In this comparison, slight improvements in overall accuracy are reported from the CASI sensor over those obtained using the Landsat TM sensor. Further improvements were obtained using the AVIRIS sensor, with the maximum accuracy on the order of 90% across all cover types for this particular landscape. Within a given sensor, variation in the reported accuracy can result from any of several factors, including the particular algorithms or bands used (more

bands generally being better) and different overpass dates (Fig. 3). In this comparison, it appears that the increased accuracy over time can be partly attributed to the increased information (e.g., greater spatial and spectral detail) available with these hyperspectral sensors (Fuentes et al., 2001), although other effects cannot be ruled out. It is likely that the highest accuracy (roughly 90% across all test pixels) represents a theoretical limit using this particular assessment method. This further supported by the accuracies of  $\sim 90\%$  obtained by Beaubien et al. (1999, 2000) for 28 detailed land-cover classes over the entire BOREAS region. The roughly 10% error remaining may be unavoidable due to errors in the remotely sensed product, errors in the SERM map used for accuracy assessment, and the imperfect co-registration of the two (Fuentes et al., 2001).

A number of multidirectional sensors, including (1) the Advanced Solid-state Array Spectroradiometer instrument (ASAS; Russell, Irons, & Dabney, 1997; Sandmeier & Deering, 1999), (2) the Portable Apparatus for Rapid Acquisition of Bidirectional Observations of Land and Atmosphere instrument (PARABOLA; Li, Moreau, Cihlar, & Deering, 1997), and (3) the Polarization and Directionality of Earth Reflectances instrument (POLDER; Bicheron, Leroy, Hauteceur, & Br  on, 1997) were used in BOREAS primarily to characterize the bidirectional reflectance distribution function (BRDF). While the primary applications were to characterize the structural and radiative properties of boreal stands, a fortuitous by-product of these studies was

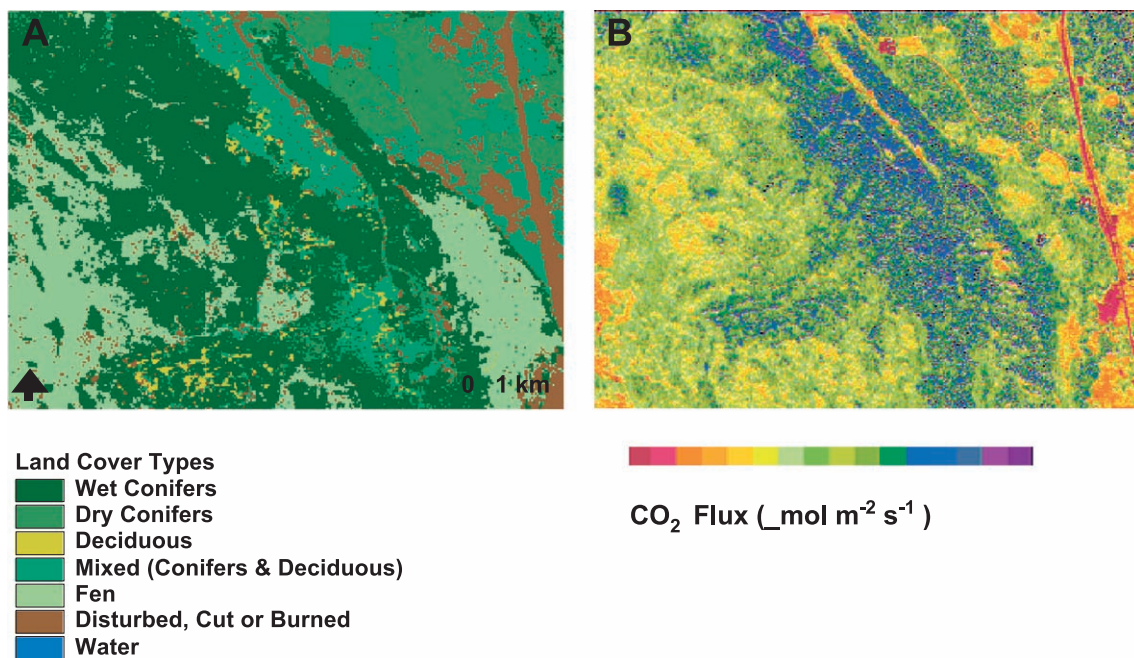


Fig. 4. Comparison of land-cover types (A) with midday gross carbon uptake rates (2-h averages near solar noon) derived from AVIRIS imagery for a portion of the SSA. The land-cover types were derived from pigment and water absorption features using a combination of spectral mixture analysis and a maximum likelihood classification (Fuentes et al., 2001). The  $\text{CO}_2$  flux image (B) was derived from NDVI and scaled PRI using a light-use efficiency model and provided an empirically calibrated regional image of midday fluxes for September 16, 1994. This method yielded a strong agreement ( $r^2 = 0.8$ ) with fluxes determined by eddy covariance from five different boreal ecosystems (Rahman et al., 2001).



the confirmation that BRDF signatures vary predictably with the dominant land-cover types, offering a novel means of mapping vegetation for the boreal forest region (see Russell et al., 1997; Sandmeier & Deering, 1999). Furthermore, the specular component of the BRDF helps isolate inundated areas such as fens (e.g., Vanderbilt et al., 2002), which are important regional sources of methane.

A further example of enhanced dimensionality applied to vegetation mapping was provided by the synergistic combination of radar and optical (e.g., TM or AVIRIS) data, which integrates the power of radar for structural analyses with the additional information present with optical sampling. For example, shuttle imaging radar (SIR-C/XSAR) and Landsat imagery was used by Ranson et al. (1997) to map seven land-cover classes as well as biomass over a portion ( $80 \times 20 \text{ km} = 1600 \text{ km}^2$ ) of the smaller modeling sub-area (MSA) within the SSA. The SIR-C L-band and the NIR and SWIR Landsat TM bands contributed the most information content to the classifier, with 87% accuracy obtained for a sample of 62 field plots using a standard supervised maximum likelihood approach. Good results were obtained for estimating biomass density using this integrated radar-optical data set. Ranson and Sun (2000) combined SAR and Landsat TM data to obtain classification accuracies between 72% and 84% for subsets of the BOREAS SSA, reducing classification errors occurring with radar or TM alone. When combining SAR and TM scenes from two dates, the accuracy improved to 89%. The structural information accessible with radar (Ranson & Sun, 2000; Ranson et al., 1997; Treuhaft & Siqueira, 2000) suggests that this method may prove to be particularly useful for distinguishing contrasting stand age, biomass density, and level of disturbance. Because of the impact of stand age on productivity (Ryan & Yoder, 1997; Yoder, Ryan, Waring, Schoettle, & Kaufmann, 1994), this information will be essential to refining regional carbon budget estimates, particular given the large areas of disturbed and aggrading forest (Hall et al., 1997; Steyaert et al., 1997).

Since land-cover products provide a foundation for most spatially distributed ecosystem carbon flux assessments, the wide array of novel BOREAS land-cover products now offer the potential for improved regional analyses of carbon exchange. Although most analyses of boreal carbon flux to date have not yet considered this new land-cover information, some initial applications of new remote sensing products to the carbon question are discussed next.

#### 4.3. Assessment of the carbon balance

Is the boreal forest a source or a sink of carbon, and how will global climate change affect the boreal forest carbon balance? This critical question remains difficult to answer, in part because net  $\text{CO}_2$  flux is a small sum of two large terms: photosynthetic carbon uptake and respiratory carbon loss. The error in the determination of either of these

components easily exceeds the measured values of net carbon exchange (Goulden, Munger, Fan, Daube, & Wofsy, 1996; Moncreiff, Malhi, & Leuning, 1996), particularly for low-productivity ecosystems such as the boreal forest. Consequently, while the controls on the separate photosynthetic and respiratory fluxes are largely understood, the exact magnitude of the fluxes remains only partly understood (Hall, 1999).

The large boreal carbon stores could have a large impact on the global carbon cycle. The relatively low nutrient cycling rates at high latitudes result in relatively high long-term boreal carbon storage rates averaging roughly  $30\text{--}50 \text{ g C m}^{-2} \text{ year}^{-1}$  (Harden, Sundquist, Stallard, & Mark, 1992), a result of relatively high root turnover from trees, shrubs, and mosses with relatively low decomposition rates. Over the past few thousand years, these below-ground storage processes have created a large and potentially mobile reservoir of carbon in the peatlands and permafrost areas of the boreal ecosystem. Given the large boreal carbon pools and the enormous areal extent of this ecosystem, roughly 20 million  $\text{km}^2$  (Sellers et al., 1997), relatively small shifts in carbon flux can readily lead to significant changes in atmospheric carbon levels. Such changes could result from climate change altering ecosystem respiration and primary productivity, hence altering carbon exchange between the boreal ecosystem and atmosphere. Additionally, changes in the balance of disturbance and recovery rates from fire and logging could critically affect the ecosystem carbon balance.

Remote sensing has provided key insights into these issues and undoubtedly will contribute to provide additional answers. Combined aircraft flux and remote sensing has confirmed a strong spatial correlation between vegetation greenness and  $\text{CO}_2$  flux for this biome (Desjardins et al., 1997; Ogunjemiyo, Schuepp, Desjardins, & MacPherson, 1997). Additionally, remote sensing has been used to characterize and quantify cover types and functionally important surface characteristics, including biomass density, canopy structure, and the degree of disturbed and aggrading land, all of which influence surface-atmosphere fluxes. With this information, we can now evaluate how well the flux tower footprint represents a given region, an essential step in extrapolating from point tower data to regional assessments. Additionally, novel indices and stand characterizations provided by new sensors offer more direct ways of assessing carbon stocks as well as the individual photosynthetic and respiratory component of net ecosystem exchange.

One example of a new product is the photochemical reflectance index (PRI). At the leaf and canopy scales, this index follows the activity of xanthophyll cycle pigments and thus provides a measure of photosynthetic light-use efficiency (Gamon, Serrano, & Surfus, 1997). At larger spatial scales, this index can also be strongly influenced by other factors, including seasonally changing carotenoid/chlorophyll levels (Gamon, Field, Fredeen, & Thayer,

2001; Sims & Gamon, 2002; Stylinski, Gamon, & Oechel, 2002) and canopy structure (e.g., Barton & North, 2001), both of which can be linked to stand-level photosynthetic rates and light-use efficiency. The utility of this index as a measure of stand-scale photosynthetic activity in natural ecosystems had not been fully explored prior to BOREAS largely due to the scarcity of appropriate stand-scale optical and flux measurements. With BOREAS, the availability of suitable hyperspectral data, along with flux and micrometeorological sampling at comparable spatial scales allowed a rare opportunity for the evaluation of stand-level PRI across dates and vegetation types. Remarkably, this index was well-correlated with estimates of whole-ecosystem photosynthetic light-use efficiency from BOREAS flux towers (Nichol et al., 2000). Further work demonstrated that PRI derived from AVIRIS data was strongly correlated with gross carbon flux of the major boreal ecosystems, and that combination of PRI with NDVI provided a method for mapping photosynthetic carbon gain from this biome (Rahman, Gamon, Fuentes, Roberts, & Prentiss, 2001) (Fig. 4).

The production of calibrated flux images from hyperspectral sensors (Fig. 4) allowed an evaluation of the extent to which tower fluxes are representative of the carbon flux of the larger region. One conclusion of this analysis was that the tower flux data, which have provided the foundation for the discussion of the regional carbon balance, appear to be underestimating gross carbon uptake of the SSA region by about 10% due to the tendency to locate flux towers at mature and uniform stands rather than at aggrading or mixed stands (Rahman et al., 2001). This result is in qualitative agreement with another recent study comparing GOES satellite data to tower flux measurements of energy balance (Gu, Smith, & Merritt, 1999) that concluded flux towers underestimate the regional sensible and latent heat flux by 15%. Together, these studies illustrate the utility of integrating remote sensing with flux tower sampling for identifying potential biases in the flux measurements. Given the conclusion, largely from tower flux analyses, that the boreal forest is approximately in carbon balance (Hall, 1999; Sellers et al., 1995), and given the abundance of disturbed and aggrading sites (Hall et al., 1997; Steyaert et al., 1997), this possible underestimation of measured carbon uptake suggests that the boreal forest may be a greater carbon sink than tower measurements indicate.

By combining remote sensing from several sensors with models, historical information, and flux towers, a more comprehensive picture of boreal forest carbon sources and sinks is starting to emerge. Surface parameters derived from remote sensing provide key inputs to models for mapping carbon source and sink distributions. Chen, Ju et al. (in press), Chen, Liu, Leblanc, Lacaz, and Roujean (in press) recently developed a technique to track retrospectively the historical NPP variation and soil carbon dynamics in each pixel using NPP values in recent years, forest age, and historical climate data under an assumption of

preindustrial dynamic equilibrium in the carbon cycle. They first calibrated their model using BOREAS and other tower flux data and then produced a carbon source and sink map for all of Canada's forests (Fig. 5). The BOREAS region was found to be a source of carbon during the 1990s because of the increase in fire disturbance, but Canada's forests overall acted as a small sink of about  $0.35 \text{ Tg C year}^{-1}$  in the same period. This analysis illustrates the danger of extrapolating from a single set of points to a larger region and the necessity of integrating remote sensing with other methods and sources for a synoptic view of carbon dynamics.

Remote sensing provides maps of vegetation type and key biophysical parameters (e.g.,  $F_{\text{PAR}}$  and LAI) that continue to be essential inputs to any spatially distributed analysis of carbon flux. Most regionally based analyses to date have employed AVHRR or TM products (e.g., Beaubien et al., 1999; Goetz et al., 1999; Hall et al., 1997; Liu, Chen, Cihlar, & Chen, 1999; Steyaert et al., 1997). During BOREAS, the use of both passive and active optical remote sensing to identify disturbance and monitor biomass recovery from disturbance were developed and demonstrated. Cihlar et al. (1997), Hall et al. (1997), and Steyaert et al. (1997) demonstrated the use of Landsat and AVHRR data to map fire and logging disturbance. Hall et al. developed physically based methods to estimate biomass density using a radiative transfer model to estimate canopy cover fraction from Landsat bands then biomass density and LAI by computing a theoretical relationship based on allometric relations between canopy cover fraction, biomass density, and LAI. Their technique produced biomass estimates in needle-leaf evergreen canopies with an error of less than  $\pm 3 \text{ kg m}^{-2}$  for black spruce stands ranging in biomass from 1 to  $12 \text{ kg m}^{-2}$  (Hall et al., 1997). This approach was subsequently used by Asner, Bateson, Privette, ElSaleous, and Wessman (1998) to estimate vegetation structural effects on carbon uptake.

Newer remote sensing products from radar, multiple-view-angle, laser altimetry, or hyperspectral sensors offer improved surface characterization. Radar, in particular, offers the potential for frequent (e.g., daily), circumpolar monitoring of boreal regions due to its virtual all-weather capability regardless of solar illumination or cloud cover conditions. While initial results for many of these new technologies show promise, their potential to improve carbon models remains largely untested.

Insight into interannual patterns of carbon flux has been obtained from radar backscatter data, which is uniquely capable of penetrating cloud cover. Exploration of freeze–thaw dynamics from radar backscatter revealed a relatively simple method for characterizing spring thaw and fall freeze (Fig. 6) (Frolking et al., 1999; Kimball, McDonald, Frolking, & Running, 2003). Variation in freeze/thaw dates are believed to have a large influence on the annual carbon balance of northern latitude forest (Goulden et al., 1997) and could prove to be one of the most sensitive indicators

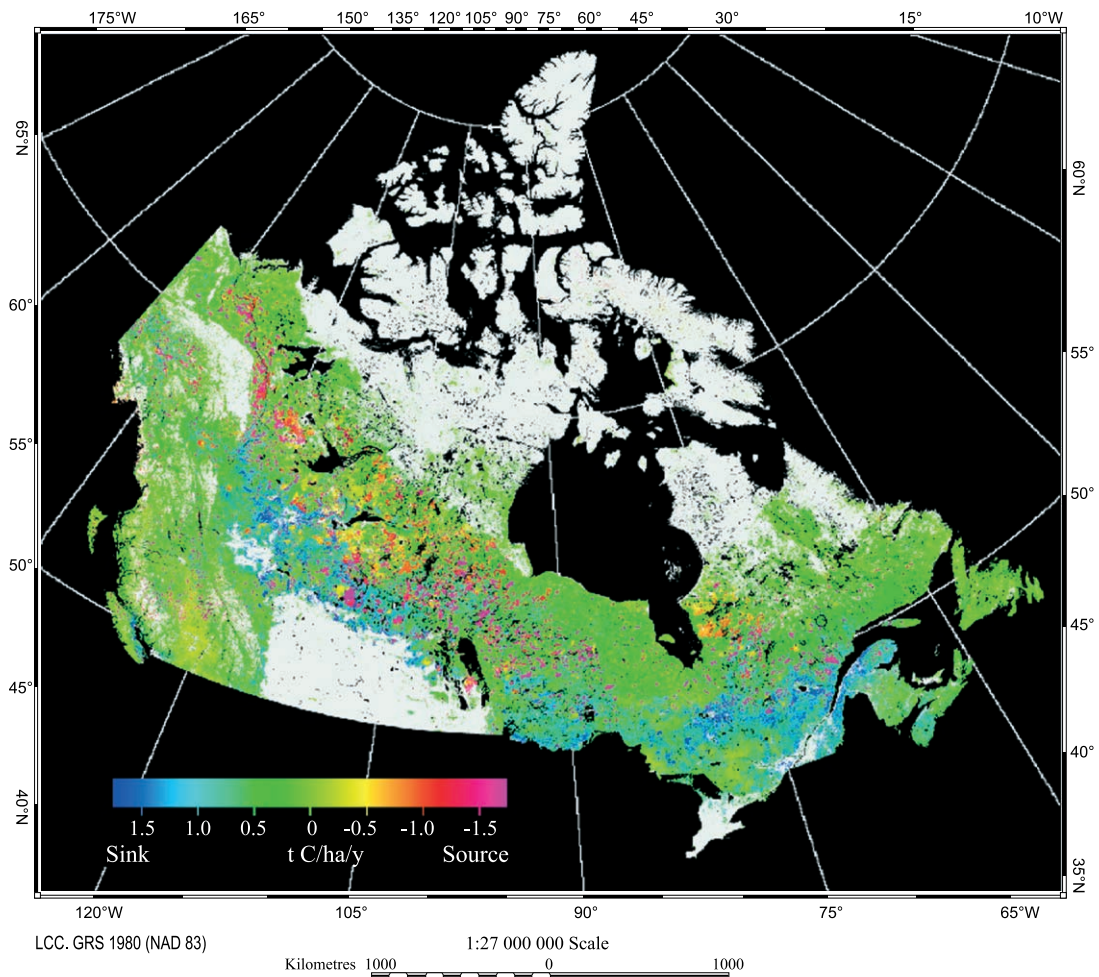


Fig. 5. Carbon source and sink distribution in Canada's forests for the period 1990–1998, in terms of net biome productivity, which includes carbon absorption by vegetation, releases from soils due to decomposition of dead organic matter, and direct carbon emission during fires. White color indicates nonforested areas. Source: Chen, Ju et al. (2003), Chen, Liu et al. (2003). (a) ERS-1 SAR landscape freeze–thaw classification. (b) ERS-1 SAR backscatter comparison with vegetation temperature and snow depth.

of biospheric responses to global climate change (Myneni, Keeling, Tucker, Asrar, & Nemani, 1997). Similarly, multi-temporal AVHRR analyses (Myneni et al., 1997; Tucker et al., 2001) suggest that northern latitudes may be experiencing earlier spring greening. However, it should be noted that the sampling period of some sensors (e.g., AVHRR) lacks the temporal resolution to conclusively resolve subtle temporal differences. While the advent of MODIS products at 8-day intervals (Myneni et al., 2002) offer opportunities to further improve our understanding of interannual vegetation dynamics, the integration of radar backscatter measurements with the global NDVI products could go a long way towards pinpointing subtle differences in season length and thus clarify regional changes in carbon balance.

An important component of the forest carbon cycle is the stock of carbon in woody biomass. Polarimetric radar data from AIRSAR were used to estimate biomass of the southern study area (Saatchi & Moghaddam, 2000) and thus may be useful for mapping carbon stocks. In this study, the best accuracy (over 90%) was achieved by

including multiple frequencies and polarizations, with the accuracy degrading gradually as the variety of channels decreased. Other instruments such as lidar have also been recognized for estimating biomass through relating vegetation height profiles to biomass (e.g., Lefsky, Harding, Cohen, & Parker, 1999). An active optical sensor (SLICER—Scanning Lidar Imager of Canopies by Echo Recovery) flown on aircraft demonstrated the potential for lidar estimates of biomass density (Lefsky et al., 2002). They compared the relationships between lidar-measured canopy structure and coincident field measurements of above-ground biomass at sites in the BOREAS black spruce canopies as well as in temperate deciduous and temperate coniferous canopies. A single regression for all three sites explained 84% of variance in aboveground biomass ( $p < 0.0001$ ) and showed no statistically significant bias in its predictions for any individual site.

Radar algorithms for biomass and vegetation variable estimation rely on ancillary information to help establish correlations between canopy geometrical parameters. For



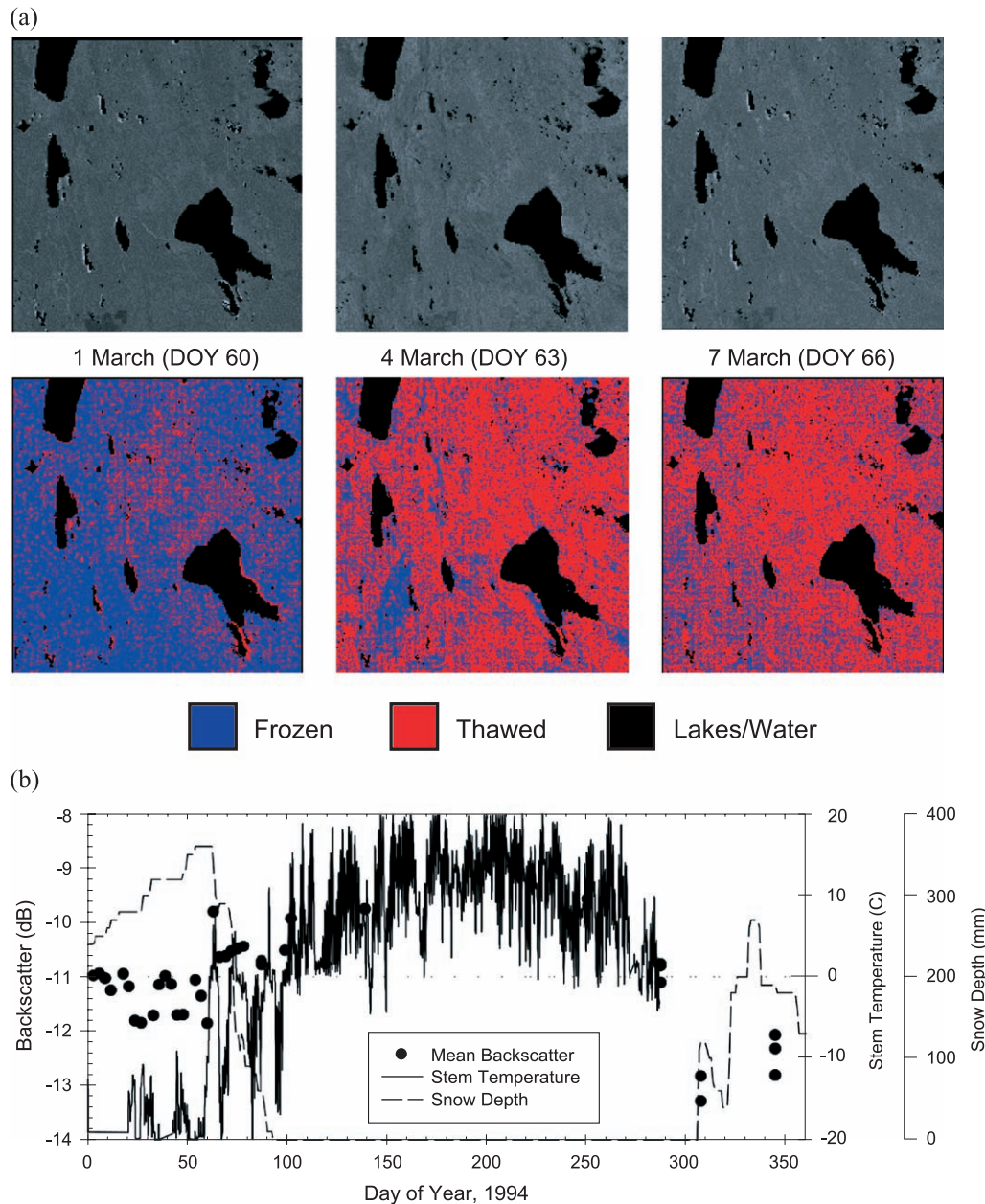


Fig. 6. (a) Sequence of ERS Synthetic Aperture Radar backscatter images (top row) and corresponding classifications (second row) for three dates in 1994 (day of year also indicated) in the BOREAS SSA, illustrating the radar's ability to monitor thaw processes related to the start of growing season and initiation of photosynthetic processes in the vegetation. (b) ERS-1 SAR backscatter from the SSA Old Black Spruce site compared with tree stem temperature and snow depth.

example, knowledge of vegetation class type and/or allometric relations are needed. Therefore, combining radar data with other data types (multispectral or hyperspectral optical with field validation) is needed to ensure success of the radar algorithms. Indices from optical sensors (e.g., NDVI or the indices of foliar water content) are often strongly related to total stand biomass, but these relationships can be confounded by seasonally varying leaf display or other factors and, thus, do not always provide reliable measures of biomass. Thus, it appears that combinations of sensors and data sources may be the best way to yield accurate biomass estimates.

A primary use of remote sensing has been to derive parameter fields for regional estimates of net primary production (NPP), an expression of annual ecosystem carbon gain. Major conclusions from these efforts are that spatially extensive lowland conifer (e.g., black spruce) areas are less productive than the less common deciduous forests or croplands, and that interannual variability in boreal carbon uptake is considerable, largely linked to the timing of the spring thaw (Goetz et al., 1999; Kimball, Keyser, Running, & Saatchi, 2000; Liu et al., 1999). Good agreement (within 10–30%) in relative magnitudes and season-



ality between modeled and measured carbon fluxes across several key land-cover types (Goetz et al., 1999; Kimball et al., 2000) provides some degree of confidence in these regional NPP estimates.

Radar data offers considerable promise for improving NPP estimates. For example, polarimetric multifrequency AIRSAR data have been used to systematically derive top-to-bottom vegetation canopy variables, including crown layer moisture content, crown layer depth, stem moisture content, soil moisture, and stem density (Moghaddam & Saatchi, 1999; Moghaddam, Saatchi, & Cuenca, 2000). Because of the varying degrees of penetration of multifrequency radar signals into vegetation canopies, it was possible to devise an algorithm that uses successively decreasing frequencies to characterize deeper layers of the vegetation canopy. Multiple AIRSAR data acquisitions from April to September 1994 were used to generate crown and soil dry-down maps of part of the SSA using this algorithm. The temporal variation in these values could be used to replace constants that are currently used to drive biogeochemical models for assessing NPP, possibly improving NPP estimates.

#### 4.4. Links between surface properties, weather, and climate

The representation of land surface processes in numerical weather prediction and climate models is generally undertaken by the implementation of some type of soil–vegetation–atmosphere transfer scheme (i.e., a SVATS process model) that is capable of describing mass and momentum flux exchanges at the interface between the surface and

atmosphere (i.e., at the base of the boundary layer). An ongoing research topic in SVATS modeling is the application of satellite observations to the production of updated surface properties (e.g., LAI, surface albedo, directional-spectral fluxes defining the incoming terms of the surface radiation budget; Chen et al., 1997; Habets et al., 1999). A particularly instructive example from BOREAS is the exploration of the surface radiation budget (SRB), particularly the detailed albedo fields derived from the GOES satellite measurements (Gu & Smith, 1997, *this issue*; Gu et al., 1999).

Over the boreal forest zone, surface albedo is highly dependent on latitude and season, as illustrated in Fig. 7 (from Gu & Smith, *this issue*). This latitude–time diagram is based on an analysis of GOES satellite measurements according to a retrieval methodology described in the studies of Gu and Smith (1997, *this issue*). Between the ~ 54–56°N latitude zone bounded by the BOREAS SSA and NSA, where nearly all recent understanding of the relatively dark albedo properties of the boreal forest has been drawn, wintertime albedos are at their minimum, ranging from approximately 0.2–0.3 (see also figure 12c in Gu & Smith, 1997). (Note that Betts & Ball, 1997 found individual site wintertime albedos as low as 0.11 for conifers.) Across the entire 50–60°N latitude zone, forests are denser with respect to zones to the north and south and usually warmer than the zone to the north. Because wintertime winds at these latitudes are strong, snow that initially is intercepted by tree branches (approximately 90% of total snowfall) is relatively quickly removed (within 3 days) by a combination of sublimation

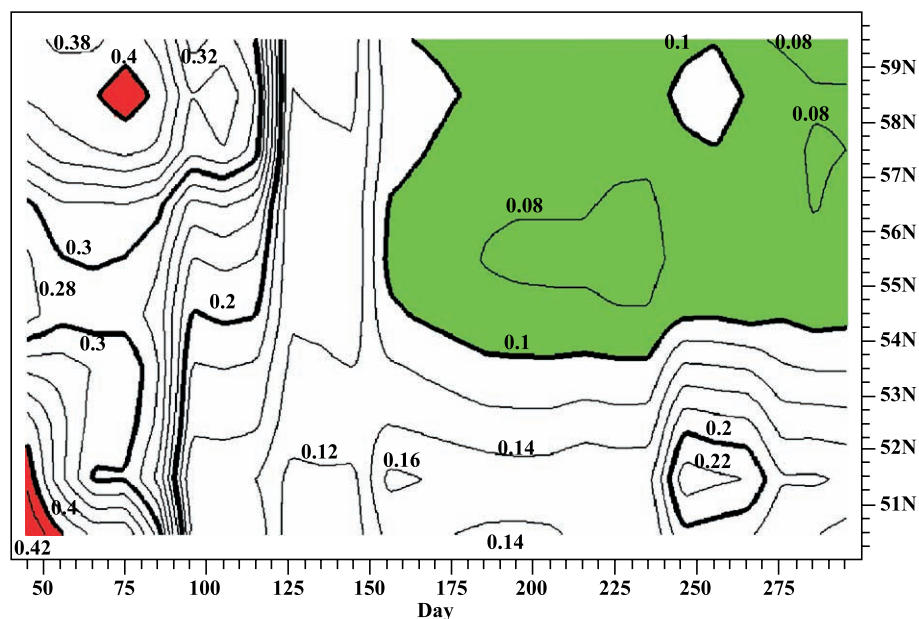


Fig. 7. Latitude–time cross-section of broadband surface albedo derived from GOES satellite measurements over study area bounded by 50–60°N/97–107°W from days 45–295, 1996 (February 14–October 22).

and unloading (blow-off) at a ratio of about 2:1 (see Pomeroy & Schmidt, 1993; Hedstrom & Pomeroy, 1998; Pomeroy, Parviainen, Hedstrom, & Gray, 1998). This results in exposed forest canopies which reduces surface albedo relative to the case for a prolonged snow-covered canopy.

The highest boreal latitudes analyzed in Fig. 7 are colder with sparser forest cover, exhibiting wintertime albedos in the 0.3–0.4 range. At central boreal latitudes where the densest forests predominate, wintertime albedos are lower by approximately 0.1. At the lowest boreal latitudes where the forest starts transitioning into prairie and agricultural lands (landscapes which tend to retain snow cover), wintertime albedos are once again elevated to the 0.3–0.4 range. As winter transitions into summer, albedos reduce to their minimum values in the 0.08–0.1 range with a much different structure in latitudinal variation. The lowest albedos of the mixed forest zone north of 54°N gradually change to values between 0.1 and 0.2 in the southern zone where there are extensive cultivated lands, particularly grain croplands south of 52°N (Steyaert et al., 1997). From this work, an improved understanding of the annual cycle of surface albedo across the boreal forest zone was gained, as well as a better recognition of its variability and complexity.

At many times during the growing season, the lower forest albedos combine with relatively low evapotranspiration and photosynthetic rates characteristic of northern evergreen forests to tightly control surface-atmosphere carbon, water, and energy exchanges (Baldocchi et al., 2000; Gu et al., 1999; Sellers et al., 1995). Because of the concomitant relatively high sensible heat fluxes required for surface energy balance, especially in spring and in dry periods, such conditions can promote the development of deep, dry atmospheric boundary layers associated with semiarid zones and deserts, reinforcing the notion of the boreal forest as a “green desert” (Betts, Ball, & McCaughey, 2001).

These GOES SRB retrievals were combined with additional in situ meteorological surface observations (pressure, temperature, humidity, wind speed–direction) and rainfall to create a 3-year continuous radiation–meteorology–precipitation forcing data set used for a hydrometeorological (hydromet) model intercomparison study (Table 5) that is nearing completion (Eric Wood, personal communication, 2002). A key finding of this hydromet model intercomparison is that the use of this common forcing data set leads to very good agreement between the models insofar as the available heating term (i.e., net radiation flux plus soil heat flux). As a result of this agreement, there is also very good agreement among the component sensible and latent heat flux terms. A significant exception is that each of the models uses a different approach for specifying wintertime snow albedo, which has the expected result of creating model disagreement concerning snow ablation and melt off.

Table 5

Identification of institutions and participants of BOREAS hydromet model intercomparison project

Model	Institution	Participants
1	European Center for Medium Range, Weather Forecasting (ECMWF)	Alan Betts
2	Florida State University (FSU)	Eric Smith, Harry Cooper, Jiuqing Gu, James Lamm
3	National Center for Atmospheric Research (NCAR)	Gordan Bonan, Keith Oleson
4	Princeton University/ University of Washington (PU-UWASH)	Eric Woods, Dennis Lettenmaier, Bart Nijssen, Valentijn Pauwels
5	University of Arizona (ARIZ)	Robert Dickinson, Jean Morrill, Kaye Schaudt
6	University of Waterloo (UWAT)	Eric Soulis, Nicholas Kouwen, Kenneth Snelgrove, Edward Whidden

A second conclusion emerging from the hydromet model intercomparison is that high space–time resolution satellite precipitation information would have greatly improved our understanding of the water budget. This is because precipitation forcing information was derived from objectively analyzed rain and snow gauge measurements, and large regions of the study area (mostly in the northern half) had insufficient gauge density to take advantage of the underlying spatial resolution in the meteorological and SRB forcing data. In the wintertime, snow gauge reports were too few to provide a sufficiently detailed picture of the wintertime water budget throughout the large-scale domain.

In part due to these limitations, two model run iterations were required to obtain good agreement between the various sets of model results. Until the BOREAS hydromet intercomparison, satisfactory model convergence of SVATS models had not been achieved—such as found with the SVATS model intercomparisons of the Project for Intercomparison of Land-Surface Parameterization Schemes (PILPS), as described in Henderson-Sellers, Pitman, Love, Irranejad, and Chen (1995) and Pitman and Henderson-Sellers (1998).

The hydromet model intercomparison study of BOREAS has led to additional nomenclature for SVATS modeling, that being the term “hydrometeorological model” denoting the need for fully integrating detailed SVATS and hydrology sub-models to obtain representative model simulations of surface radiation, heat, and water budgets, all of which are intrinsically connected. In this same sense, an important outcome of having the BOREAS science team conduct separate surface hydromet and carbon model intercomparison studies is the recognition that integrating detailed carbon cycle-driven CO<sub>2</sub> assimilation and respiration processes into hydrometeorological energy-balance models is just as important as integrating detailed surface energy budget-driven radiation, heat, water, and momentum processes into carbon balance models. (A detailed analysis of the BOREAS carbon model intercomparison study results is

provided in Amthor et al., 2001; Potter et al., 2001.) Therefore, it is clear that the next generation of climate models will require fully coupled and physically integrated hydrometeorological and carbon assimilation–respiration process models.

Clearly, remote sensing science in BOREAS has improved our knowledge of the physical climate system. The use of frequent, large-area GOES measurements to acquire detailed knowledge of the surface radiation budget and surface albedo, along with the concomitant improvement that has taken place in hydrometeorological process models (now central components of all prognostic climate models) afforded by the BOREAS hydromet model intercomparison project, is just one example of how such improvements have evolved. Notably, during the snow melt period when snow surface metamorphosis is rapid and with albedo being sensitive to snow surface structure and forest cover properties, determination of turbulent heat and moisture fluxes and understanding of how to model albedo more accurately and explicitly can be greatly aided by improved remotely sensed albedo quantities. Improved spatial, spectral, and angular resolution offered by new satellite sensor systems such as those on board the current TERRA and AQUA sun synchronous satellites and the METEOSAT Second Generation (MSG) geosynchronous satellite, as well as the planned sensors for the next-generation operational NPOESS satellite platforms, will allow more refinements to broadband albedo retrievals because of anticipated improved corrections for spectrally differential atmospheric attenuation and improved BRDF formulations.

Moreover, BOREAS has been successful in clarifying the contribution of multi-scale and directional radiative effects necessary to improve radiation schemes in climate models (Bicheron et al., 1997; Li et al., 1997; Russell et al., 1997; Sandmeier & Deering, 1999). Scaling strategies consisting of comparing remotely sensed radiances from tower scale to patch scale and finally to regional scale (including water bodies) are leading to a new generation of radiative transfer models which account for grouping effects across scales. This research will enable better representation of canopy clumping effects on the radiation field and thus avoid energetic biases in weather and climate models due to applying simplifying assumptions concerning homogeneous media and isotropic radiation. In this context, the multi-angular radiation observation program of BOREAS has enabled a better definition of the radiation field inside a forest biome, thereby providing a better quantitative representation of the radiative flux divergence across vertical layers. This representation is essential to accurately calculating diabatic radiative heating and cooling processes within and just above a forest canopy. The potential of BRDF information for improving land-cover type mapping and for enhancing our understanding of the exchange of mass and energy in the boreal forest biome is beginning to be explored (Chen, Ju et al., in press; Chen, Liu et al., in press; Privette, Eck, & Deering, 1997). It is now apparent

that surface representations in hydrometeorological models need to account for anisotropy due to the occurrence of gaps in the canopy, which reduces albedo relative to a horizontally homogenous canopy distribution. This becomes particularly critical when considering the reflectance effect of snow beneath a forest canopy (e.g., Betts, Viterbo et al., 2001; Viterbo & Betts, 1999).

There are remaining challenges in improving the links between the physical climate system and surface properties and processes, as well as how canopies intercept precipitation and retard rain flux to the ground. Remote sensing has an important role to play in understanding these processes, just as it has already had on arriving at a better definition of the variability of wintertime albedos across the large scale boreal forest ecosystem. Other climate modeling problems having to do with heat transfer between the ground surface and canopy, the heat capacitance of the canopy, and the partitioning between latent and sensible heat flux within the canopy and across the canopy–atmosphere interface are also “frontier” issues that new strategies in remote sensing will address.

## 5. Recommendations

To spur additional advances, we recommend further development in six particular directions: (1) comparative approaches, (2) intermediate-scale sampling, (3) multidimensional sampling, (4) stand structure, (5) integration between remote sensing and modeling, (6) increased attention to respiration, and (7) informatics.

### 5.1. Expand comparative approaches

The “classic” experimental method, with comparison between treatments and controls and ample replication, is rarely adopted for large landscapes. Greater inclusion of ecosystem manipulations and comparative analyses in remote sensing campaigns would significantly increase the utility of remotely sensed data. As with most ecosystem experiments, BOREAS primarily adopted a representative approach, largely because of the prohibitive cost of a fully replicated, experimental approach at this scale. To the extent that they were adopted, comparative approaches provided valuable insights into the function of this biome. For example, the analysis of successional stages revealed that disturbance alters respiration, albedo, seasonal extent, and patterns of carbon gain (e.g., Figs. 4 and 5). Clearly, continued analysis of mature, aggrading, and disturbed sites would yield further insights into the temporal and spatial dynamics of carbon for this ecosystem. Recent studies have attempted to evaluate disturbance by considering fire effects or by sampling chronosequences with flux towers (e.g., Litvak, Miller, Wofsy, & Goulden, in press). Remote sensing could help these efforts by examining how representative these flux locations are and by extrapolating to the larger region. Another needed experimental approach would

be to evaluate the sensitivity of carbon or climate models to a wider variety of remote sensing science products. Most model runs are based on a single set of land cover or biophysical parameters (e.g., derived from AVHRR or Landsat TM), without evaluating the potential impact of novel, alternative products on the resulting model output. For example, many of the newer structural characterizations attainable using hyperspectral, multiangle, radar, and lidar sensors could be compared to single-angle, broadband products derived from AVHRR, Landsat TM, or MODIS. Similarly, models could explore the impact of various LAI products or land-cover products on overall regional climate or carbon gain. For these analyses, further studies could take advantage of the rich array of remote sensing products already available ([http://www-eosdis.ornl.gov/BOREAS/boreas\\_home\\_page.html](http://www-eosdis.ornl.gov/BOREAS/boreas_home_page.html)).

### 5.2. Develop intermediate-scale sampling protocols

Much of the progress in BOREAS was made by ground-based or low-flying platforms, which are intermediate in scale between most field measurements and satellite remote sensing. These platforms are generally considered “experimental” and are often not favored by funding agencies because of their relatively high cost. However, BOREAS demonstrated the value of these approaches. Direct connections between variables measured in the field and remotely sensed signals from aircraft were possible because of their intermediate scale and flexible deployment. If we are to continue to make fundamental progress with remote sensing, ongoing support for such platforms (e.g., in the form of drones and/or low-flying aircraft) and innovative field sampling methods will be essential. Many of these methods need not be particularly expensive to be effective. For example, Huemmrich, Black, Jarvis, McCaughey, and Hall (1999) demonstrated the utility of continuous NDVI measurements from existing flux tower meteorological sensors for capturing phenology linked to carbon flux. Because carbon flux varies in time, it cannot be readily captured by the “single snapshot” approach of most remote sensing, which is often ill-equipped to match the temporal and spatial scale of field sampling. Further development of such low-cost, mid-scale sampling protocols could be of great use in validating measured and modeled satellite products.

### 5.3. Develop multidimensional sampling

Continued exploration of the multidimensional aspects of remote sensing are likely to further improve characterization of surface properties and processes. This includes consideration of temporal dynamics, multiple-view-angle, hyperspectral, and synergistic combinations of sensors (e.g., optical, lidar, and radar). For maximum utility, these studies should include direct, quantitative comparisons between multidimensional products and single-sensor or single-dimensional products. Radar estimation algorithms produce

progressively better results as more frequencies and polarizations are included in the analyses, and best results were obtained when integrated with other data such as Landsat TM (Saatchi & Moghaddam, 2000) as well as with in situ measurements and interferometric SAR data. Unfortunately, little has been done in combining radar polarimetry and interferometry for BOREAS, mainly because of the limited and inconsistent INSAR data (the one INSAR flight line was not coincident with any other AIRSAR flight lines in BOREAS). In the future, this problem can be avoided by planning consistent flight lines for all instruments involved. To maximize information content, INSAR acquisitions for vertical structure characterization should be done with multiple baselines and in conjunction with other remote sensing devices.

### 5.4. Refined assessment of stand structure

Most current ecosystem carbon flux models use reported values of NDVI, APAR, and LAI without much critical evaluation or consideration of the full meaning and dynamics of these parameters. The issue of LAI (as traditionally defined) vs. “effective LAI” (as defined by new optical sensors) needs further examination and definition. Similarly, the complexities of forest stand structure and how it influences absorbed photosynthetically active radiation (APAR) and NDVI need further attention. During BOREAS, we learned that many traditional applications of LAI and APAR are not particularly meaningful given the highly clumped and two-layered structure of many boreal stands. Novel remote sensing methods and products (e.g., Chen, Ju et al., *in press*; Chen, Liu et al., *in press*; Hu et al., 2000; Lacaze et al., 2002; Rapalee et al., 2001; Sandmeier & Deering, 1999) are now contributing to improved characterization of complex stands. These methods and products need to be further developed, tested, standardized, and more widely adopted to realize their full utility.

### 5.5. Integrating remote sensing with models

Better integration of remote sensing with other disciplines (e.g., hydrometeorological and carbon cycle modeling) is clearly a priority. A unique aspect of BOREAS was the relatively close interaction and coordination among remote sensing, fieldwork, and modeling teams. Remote sensing advances during BOREAS were often initiated in direct response to the specific needs of field and modeling teams. For example, advances in remote sensing-based land cover, age class, and canopy structure discrimination were developed largely in response to the need for improved regional SVATS model parameterizations to better reflect field-based observations. Interactions among these groups facilitated a better understanding of the potential use and limitations of remote sensing. The significant advances in land cover and biophysical estimation derived from integrating radiative transfer with canopy geometric optical



reflectance models provides another example of the benefits of incorporating modeling into remote sensing efforts. Modelers should be encouraged to employ novel remotely sensed products, and remote sensing scientists should be encouraged to develop and utilize models. Wide-scale adoption and integration of new products remains a challenge, particularly since these newer products are slow in emerging and are of limited coverage. Nonetheless, a major legacy of BOREAS is the relatively rich archive of contemporaneous field measurements and multi-scale remote sensing data from multiple platforms that enable robust regional assessment and intercomparison studies of remote sensing algorithms and technology, as well as the continued development of new applications. Remote sensing products offer a means for validating model outputs, appraising the reliability of models, and providing needed model input parameters. With proper support and coverage, new remote sensing tools and their products can provide a way to monitor the outcome of the carbon exchange processes themselves (e.g., Fig. 4).

#### 5.6. Increased attention to respiration

A significant remaining need is a reliable method for estimating ecosystem respiration from remote sensing. While, at first glance, this seems like an impossible task, it is actually a reasonable goal, considering that many of the inputs to most respiration models (e.g., temperature, moisture, biomass, and soil and vegetation type) are now available via remote sensing.

#### 5.7. Enhanced informatics

There is a new age emerging in Earth System Science where massive amounts of data products are now routinely available in standardized and documented formats. BOREAS provided a laudable example of the benefits that accrue when data management and archiving receives the attention they deserve. It is imperative that funding agencies continue supporting information activities and that the culture of science continues to evolve so that scientists are encouraged to submit and fully utilize these data products.

### 6. Conclusions

BOREAS was an unprecedented exercise in field monitoring and teamwork that, in many ways, has contributed to a redefinition and refocusing of the scientific method itself. At the same time, the field of remote sensing has also evolved substantially and is now far more diverse in its goals, methods, and conclusions than before the onset of BOREAS. BOREAS stimulated many efforts to push the technology and interpretation of remote sensing into new directions, with many of these efforts continuing today. Particular successes included improved definition of vege-

tation structure and land cover for assessment of the surface–atmosphere exchange of mass and energy, the nature and variability of the surface albedo and radiation budget, and the regional carbon balance. Particular weaknesses include the lack of consistent time series data—most remote sensing remains a mapping tool rather than a tool for examining temporal processes, though this is expected to be less of a problem as data archiving and calibration efforts increase, and as more sensors are launched. However, for novel sensors, this issue is expected to remain for some time, as it is difficult and costly to apply untried approaches at the ecosystem scale at the frequency required for meaningful temporal profiles, until warranted through more extensive research validation.

BOREAS involved unusually close interaction and coordination among data management, remote sensing, modeling, and field-based activities. However, in the past, remote sensing has often existed “in the background”, providing a service role and sometimes not well-connected with other efforts (e.g., field sampling, flux monitoring, and modeling), resulting in many mismatches of space and time. Remote sensing could be far better integrated with other data systems, and this integration can be greatly assisted by adopting the team approach used in BOREAS. Key aspects of this team approach to be continued in the future might include upgraded support for coordination, logistics, and data archiving and distribution. Perhaps the greatest contribution of BOREAS is that an immense and high-quality data archive is available in a form accessible for future analyses ([http://www-eosdis.ornl.gov/BOREAS/boreas\\_home\\_page.html](http://www-eosdis.ornl.gov/BOREAS/boreas_home_page.html)). Thus, as we reach the end of the first decade of BOREAS, we anticipate that dramatic new results in remote sensing science will continue to emerge.

### Acknowledgements

Funding sources for BOREAS included NASA, the US National Science Foundation, the US Geological Survey, the US Forest Service, the US Environmental Protection Agency, the Canada Centre for Remote Sensing, Natural Resources Canada, Environment Canada, Natural Sciences and Engineering Research Council of Canada, Agriculture and Agri-Food Canada, National Research Council of Canada, Parks Canada, Canadian Forest Service, Institute for Space and Terrestrial Science (now CRESTech), Canadian Space Agency, and the Royal Society of Canada.

### References

- Amthor, J. S., Chen, J. M., Clein, J. S., Frohling, S. E., Goulden, M. L., Grant, R. F., Kimball, J. S., King, A. W., McGuire, A. D., Nikolov, N. T., Potter, C. S., Wang, S., & Wofsy, S. C. (2001). Boreal forest CO<sub>2</sub> exchange and evapotranspiration predicted by nine ecosystem process models: Intermodel comparisons and relationships to field measurements. *Journal of Geophysical Research*, 106, 33623–33648.

- Asner, P. G., Bateson, C. A., Privette, J. L., El Saleous, N., & Wessman, C. A. (1998). Estimating vegetation structural effects on carbon uptake using satellite data fusion and inverse modeling. *Journal of Geophysical Research*, 103(D22), 28839–28853.
- Baldocchi, D., Kelliher, F. M., Black, T. A., & Jarvis, P. G. (2000). Climate and vegetation controls on boreal zone energy exchange. *Global Change Biology*, 6(Suppl. 1), 69–83.
- Barton, C. V. M., & North, P. R. I. (2001). Remote sensing of canopy light use efficiency using the photochemical reflectance index: Model and sensitivity analysis. *Remote Sensing of Environment*, 78, 264–273.
- Beaubien, J., Cihlar, J., Simard, G., & Latifovic, J. (1999). Land cover from multiple thematic mapper scenes using a new enhancement-classification methodology. *Journal of Geophysical Research*, 104(D22), 27909–27920.
- Beaubien, J., Latifovic, R., Cihlar, J., & Simard, G. (2000). Land cover classification of the BOREAS Transect derived from Landsat Thematic Mapper data. Project TE-16, a contribution to BOREAS follow-on investigation, Canadian Forest Service and Canada Centre for Remote Sensing.
- Belward, A. S. (1996). The IGBP-DIS Global 1-km land cover data set (DISCover)—Proposal and implementation plans, IGBP-DIS Working Paper No. 13, Toulouse, France.
- Betts, A. K., & Ball, J. H. (1997). Albedo over the boreal forest. *Journal of Geophysical Research*, 102(D24), 28901–28909.
- Betts, A. K., Ball, J. H., & McCaughey, J. H. (2001). Near-surface climate in the boreal forest. *Journal of Geophysical Research*, 106, 33529–33541.
- Betts, A. K., Viterbo, P., Beljaars, A. C. M., & van den Hurk, B. J. J. M. (2001). Impact of BOREAS on the ECMWF forecast model. *Journal of Geophysical Research*, 106(D24), 33593–33604.
- Bicheron, P., Leroy, M., Hauteceur, O., & Bréon, F. M. (1997). Enhanced discrimination of boreal forest covers with directional reflectances from the airborne polarization and directionality of Earth reflectances (POLDER) instrument. *Journal of Geophysical Research*, 102, 29517–29528.
- Bréon, F. M., Vanderbilt, V., Leroy, M., Bicheron, P., Walthall, C. L., & Kalshoven, J. E. (1997). Evidence of hot-spot signature from airborne POLDER measurements. *IEEE Transactions on Geoscience and Remote Sensing*, 35, 479–484.
- Chen, J., & Cihlar, J. (1996). Retrieval leaf area index of boreal conifer forests using Landsat TM images. *Remote Sensing of Environment*, 55, 153–162.
- Chen, J. M., & Cihlar, J. (1995). Plant canopy gap size analysis theory for improving optical measurements of leaf area index. *Applied Optics*, 34, 6211–6222.
- Chen, J. M., Ju, W., Cihlar, J., Price, D., Liu, J., Chen, W., Pan, J., Black, T. A., & Barr, A. (2003). Spatial distribution of carbon sources and sinks in Canada's forests based on remote sensing. *Tellus-Series B-Chemical and Physical Meteorology*, 55(2), 622–641.
- Chen, J. M., & Leblanc, S. (1997). A four-scale bidirectional reflectance model based on canopy architecture. *IEEE Transactions on Geoscience and Remote Sensing*, 35(5), 1316–1337.
- Chen, J. M., & Leblanc, S. G. (2001). Multiple-scattering scheme useful for hyperspectral geometrical optical modelling. *IEEE Transactions on Geoscience and Remote Sensing*, 39(5), 1061–1071.
- Chen, J. M., Leblanc, S. G., Cihlar, J., Desjardins, R., & MacPherson, J. I. (1999). Extending aircraft and tower-based CO<sub>2</sub> flux measurements to a boreal region using a Landsat TM landcover map. *Journal of Geophysical Research—Atmosphere*, 104, 16859–16877.
- Chen, J. M., Liu, J., Leblanc, S. G., Lacaz, R., & Roujean, J. -L. (2003). Multi-angular optical remote sensing for assessing vegetation structure and carbon absorption. *Remote Sensing of Environment*, 84(4), 516–525.
- Chen, J. M., Rich, P. M., Gower, S. T., Norman, J. M., & Plummer, S. (1997). Leaf area index of boreal forests: Theory, techniques and measurements. *Journal of Geophysical Research*, 102(D24), 29429–29443.
- Chen, T. H., et al (1997). Cabauw experimental results from the project for inter-comparison of land-surface parameterisation schemes. *Journal of Climate*, 10(7), 1194–1215.
- Cihlar, J. (2000). Land cover mapping of large areas from satellites: Status and research priorities. *International Journal of Remote Sensing*, 21, 1093–1114.
- Cihlar, J., Beaubien, J., Xiao, Q., & Li, Z. (1997). Land cover of the BOREAS region from AVHRR and Landsat data. *Canadian Journal of Remote Sensing. BOREAS Special Issue*, 23(2), 163–175.
- Cihlar, J., Chen, J., Li, Z., Latifovic, R., Fedosejevs, G., Adair, M., Park, W., Fraser, R., Trishchenko, A., Guindon, B., Stanley, D., & Morse, D. (2002). GeoComp-n, an advanced system for the processing of coarse and medium resolution satellite data: Part 2. Biophysical products for northern ecosystems. *Canadian Journal of Remote Sensing*, 28(1), 21–44.
- Cihlar, J., Guindon, B., Beaubien, J., Latifovic, R., Peddle, D., Wulder, M., Fernandes, R., & Keer, J. (2002). From need to product: A methodology for completing a land cover map of Canada from Landsat. *Canadian Journal of Remote Sensing. Special Issue on Synergistic Utilisation of Landsat-7*, 29(2), 171–186.
- Cihlar, J., Xiao, Q., Beaubien, J., Fung, K., & Latifovic, R. (1998). Classification by progressive generalization: A new automated methodology for remote sensing multichannel data. *International Journal of Remote Sensing*, 19, 2685–2704.
- Czajkowski, K. P., Mulhern, T., Goward, S. N., Cihlar, J., Dubayah, R. O., & Prince, S. D. (1997). Biospheric environmental monitoring at BOREAS with AVHRR observations. *Journal of Geophysical Research*, 102(D24), 29651–29662.
- Dawson, T. P., Curran, P. J., & North, P. R. J. (1999). The propagation of foliar biochemical absorption features in forest canopy reflectance: A theoretical analysis. *Remote Sensing of Environment*, 67(2), 147–159.
- Dawson, T. P., Curran, P. J., & Plummer, S. E. (1998). LIBERTY-modeling the effects of leaf biochemical concentration on reflectance spectra. *Remote Sensing of Environment*, 65(1), 50–60.
- Deschamps, P. Y., Bréon, F. M., Leroy, M., Podaire, A., Bricaud, A., Buriez, J. C., & Sèze, G. (1994). The POLDER mission: Instrument characteristics and scientific objectives. *IEEE Transactions on Geoscience and Remote Sensing*, GE-32, 598–615.
- Desjardins, R. L., MacPherson, J. I., Mahrt, L., Schuepp, P., Pattey, E., Neumann, H., Baldocchi, D., Wofsy, S., Fitzjarrald, D., McCaughey, H., & Joiner, D. W. (1997). Scaling up flux measurements for the boreal forest using aircraft-tower combination. *Journal of Geophysical Research*, 102(D24), 29125–29134.
- Fernandes, R., Fraser, R., Latifovic, R., Cihlar, J., Beaubien, J., & Du, Y. (2003). Approaches to fractional land cover and continuous field mapping: A comparative assessment over the BOREAS study region. *Remote Sensing of Environment*, 89, 234–251 (this issue).
- Fernandes, R. A., Hu, B., Miller, J. R., & Rubinstein, I. (2002). A multi-scale approach to mapping effective leaf area index in boreal Picea mariana stands using high spatial resolution CASI imagery. *International Journal of Remote Sensing*, 23(18), 3547–3568.
- Frolking, S., McDonald, K. C., Kimball, J. S., Way, J. B., Zimmermann, R., & Running, S. W. (1999). Using the space-borne NASA scatterometer (NSCAT) to determine the frozen and thawed seasons. *Journal of Geophysical Research*, 104(D22), 27895–27907.
- Fuentes, D. A., Gamon, J. A., Qiu, H.-L., Sims, D. A., & Roberts, D. A. (2001). Mapping Canadian boreal forest vegetation using pigment and water absorption features derived from the AVIRIS sensor. *Journal of Geophysical Research*, 106(D24), 33565–33577.
- Gamon, J. A., Field, C. B., Fredeen, A. L., & Thayer, S. (2001). Assessing photosynthetic down-regulation in sunflower stands with an optically-based mode. *Photosynthesis Research*, 67, 113–125.
- Gamon, J. A., Serrano, L., & Surfus, J. S. (1997). The photochemical reflectance index: An optical indicator of photosynthetic radiation-use efficiency across species, functional types, and nutrient levels. *Oecologia*, 112, 492–501.
- Gastellu-Etchegorry, J. P., Guillevic, P., Zagolski, F., Demarez, V., Trichon, V., Deering, D., & Leroy, M. (1999). Modeling BRF and radiation regime of boreal and tropical forests: I. BRF. *Remote Sensing of Environment*, 68(3), 281–316.

- Goel, N. S., & Thompson, R. L. (2000). A snapshot of canopy reflectance models and a universal model for the radiation regime. *Remote Sensing Reviews*, 18, 197–225.
- Goetz, S. J., Prince, S. D., Goward, S. N., Thawley, M. M., Small, J., & Johnston, A. (1999). Mapping net primary production and related biophysical variables with remote sensing: Application to the BOREAS region. *Journal of Geophysical Research*, 104(D22), 27719–27734.
- Goulden, M. L., Daube, B. C., Fan, S. M., Sutton, D. J., Bazzaz, A., Munger, J. W., & Wofsy, S. C. (1997). Physiological responses of a black spruce forest to weather. *Journal of Geophysical Research*, 102(D24), 28987–28996.
- Goulden, M. L., Munger, J. W., Fan, S.-M., Daube, B. C., & Wofsy, S. C. (1996). Measurements of carbon sequestration by long-term eddy covariance: Methods and a critical evaluation of accuracy. *Global Change Biology*, 2(3), 169–182.
- Gu, J., & Smith, E. A. (1997). High resolution estimates of total solar and PAR surface fluxes over large scale BOREAS study area from GOES measurements. *Journal of Geophysical Research*, 102, 29685–29705.
- Gu, J., & Smith, E. A. (2003). GOES satellite analysis of boreal forest wintertime albedo. *Remote Sensing of Environment* (this issue).
- Gu, J., Smith, E. A., & Merritt, J. (1999). Testing energy balance closure with GOES-retrieved net radiation and in situ measured eddy correlation fluxes in BOREAS. *Journal of Geophysical Research*, 104, 27881–27893.
- Habets, F., Noilhan, J., Golaz, C., Goutorbe, J. P., Lacarrère, P., Leblois, E., Ledoux, E., Martin, E., Otlé, C., & Vidal-Madjar, D. (1999). The ISBA surface scheme in a macro-scale hydrological model applied to the HAPEX-Mobilhy area: Part 1. Model and database. *Journal of Hydrology*, 217, 75–96.
- Hall, F. G. (1999). Introduction to special section: BOREAS in 1999: Experiment and science overview. *Journal of Geophysical Research*, 104(D22), 27627–27639.
- Hall, F. G. (2001). Introduction to special section: BOREAS III. *Journal of Geophysical Research*, 106(D24), 13511–13516.
- Hall, F. G., & Knapp, D. (1994). Landsat TM maximum likelihood forest cover classification images of SSA and NSA. Greenbelt, MD: BOREAS Information System, NASA Goddard Space Flight Center.
- Hall, F. G., & Knapp, D. (1996). Landsat TM physical classification image of SSA. Greenbelt, MD: BOREAS Information System, NASA Goddard Space Flight Center.
- Hall, F. G. & Knapp, D. (1999a). BOREAS TE-18 Landsat TM Maximum Likelihood Classification of the SSA. Data set. Available online [[http://www-eosdis.ornl.gov/BOREAS/boreas\\_home\\_page.html](http://www-eosdis.ornl.gov/BOREAS/boreas_home_page.html)] from Oak Ridge National Laboratory Distributed Active Archive Center, Oak Ridge, TN, USA.
- Hall, F. G. & Knapp, D. (1999b). BOREAS TE-18 Landsat TM Physical Classification Image of the SSA and NSA. Data set. Available online [[http://www-eosdis.ornl.gov/BOREAS/boreas\\_home\\_page.html](http://www-eosdis.ornl.gov/BOREAS/boreas_home_page.html)] from Oak Ridge National Laboratory Distributed Active Archive Center, Oak Ridge, TN, USA.
- Hall, F. G., Knapp, D. E., & Huemmrich, K. F. (1997). Physically based classification and satellite mapping of biophysical characteristics in the southern boreal forest. *Journal of Geophysical Research*, 102(D24), 29567–29580.
- Harden, J. W., Sundquist, E., Stallard, R., & Mark, R. (1992). Dynamics of soil carbon during deglaciation of the Laurentide ice sheet. *Science*, 258, 1921–1924.
- Hedstrom, N. R., & Pomeroy, J. W. (1998). Measurements and modeling of snow interception in the boreal forest. *Hydrological Processes*, 12, 1611–1625.
- Henderson-Sellers, A., Pitman, A. J., Love, P. K., Irranejad, P., & Chen, T. H. (1995). The project for inter-comparison of land-surface parameterization schemes (PILPS): Phases 2 and 3. *Bulletin American Meteorological Society*, 76, 489–503.
- Houghton, J. T., Meira Filho, L. G., Callander, B. A., Harris, N., Kattenberg, A., & Maskell, K. (Eds.) (1996). *Climate change 1995: The science of climate change. Contribution of WGI to the second assessment report of the Intergovernmental Panel on Climate Change*. New York: Cambridge.
- Hu, B., Inannen, K., & Miller, J. R. (2000). Retrieval of leaf area index and canopy closure from CASI data over the BOREAS flux tower sites. *Remote Sensing of Environment*, 74, 255–274.
- Hu, B., Miller, J. R., Chen, J. M., & Hollinger, A. (2003). Retrieval of the canopy leaf area index in the BOREAS flux tower sites using linear spectral mixture analysis. *Remote Sensing of Environment*, 89, 176–188 (this issue).
- Huemmrich, K. F. (2001). The GeoSail model: A simple addition to the SAIL model to describe discontinuous canopy reflectance. *Remote Sensing of Environment*, 75, 423–431.
- Huemmrich, K. F., Black, T. A., Jarvis, P. G., McCaughey, J. H., & Hall, F. G. (1999). High temporal resolution NDVI phenology from micrometeorological radiation sensors. *Journal of Geophysical Research*, 104(D22), 27935–27944.
- Jacquemond, S., & Baret, F. (1990). PROSPECT: A model of leaf optical properties spectra. *Remote Sensing of Environment*, 34, 75–91.
- Johnson, J. D. (1984). A rapid technique for estimating total surface area of pine needles. *Forest Science*, 30, 913–921.
- Kimball, J. S., Keyser, A. R., Running, S. W., & Saatchi, S. S. (2000). Regional assessment of boreal forest productivity using an ecological process model and remote sensing parameter maps. *Tree Physiology*, 20(11), 761–775.
- Kimball, J. S., McDonald, K. C., Frolking, S., & Running, S. W. (2003). Radar remote sensing of the spring thaw transition across a boreal landscape. *Remote Sensing of Environment*, 89, 163–175 (this issue).
- Kimball, J. S., Running, S. W., & Saatchi, S. S. (1999). Sensitivity of boreal forest regional water flux and net primary production simulations to sub-grid scale land cover complexity. *Journal of Geophysical Research*, 104(D22), 27789–27801.
- Kucharik, C. J., Norman, J. M., & Gower, S. T. (1998a). Measurements of branch area and adjusting leaf area index indirect measurements. *Agricultural and Forest Meteorology*, 91, 69–88.
- Kucharik, C. J., Norman, J. M., & Gower, S. T. (1998b). Measurements of leaf orientation, light distribution and sunlit leaf area in a boreal aspen forest. *Agricultural and Forest Meteorology*, 91, 127–148.
- Kucharik, C. J., Norman, J. M., & Gower, S. T. (1999). Characterization of radiation regimes in nonrandom forest canopies: Theory, measurements, and a simplified modeling approach. *Tree Physiology*, 19, 695–706.
- Kucharik, C. J., Norman, J. M., Murdock, L. M., & Gower, S. T. (1997). Characterizing canopy nonrandomness with a multiband vegetation imager (MVI). *Journal of Geophysical Research*, 102(D24), 29455–29473.
- Lacaze, R., Chen, J. M., Roujean, J. L., & Leblanc, S. G. (2002). Retrieval of vegetation clumping index using hot spot signatures measured by POLDER instrument. *Remote Sensing of Environment*, 79, 84–95.
- Lacaze, R., & Roujean, J. L. (2001). G-function and HOT SpOT (GHOST) reflectance model: Application to multi-scale airborne POLDER measurements. *Remote Sensing of Environment*, 76, 1–14.
- Leblanc, S. G., & Chen, J. M. (2000). A Windows Graphic User Interface (GUI) for the five-scale model for fast BRDF simulations. *Remote Sensing Reviews—Special IWMMM-2 issue*, (19), 293–305.
- Lefsky, M., Cohen, W. B., Harding, D. J., Parker, G. G., Acker, S. A., & Gower, S. T. (2002). *Global Ecology and Biogeography*, 11(5), 393–399.
- Lefsky, M. A., Harding, D., Cohen, W. B., & Parker, G. G. (1999). Surface lidar remote sensing of basal area and biomass in deciduous forests of eastern Maryland, USA. *Remote Sensing of Environment*, 67, 83–98.
- Li, X., & Strahler, A. H. (1992). Geometric-optical bidirectional reflectance modeling of the discrete crown vegetation canopy: Effect of crown shape and mutual shadowing. *IEEE Transactions on Geoscience and Remote Sensing*, 30(2), 276–292.
- Li, X. W., Strahler, A. H., & Woodcock, C. E. (1995). A hybrid geometric optical-radiative transfer approach for modeling albedo and directional reflectance of discontinuous canopies. *IEEE Transactions on Geoscience and Remote Sensing*, 33(2), 466–480.



- Li, Z., Moreau, L., Cihlar, J., & Deering, D. W. (1997). An evaluation of kernel-driven bidirectional models using PARABOLA measurements. *Canadian Journal of Remote Sensing*, 23(2), 120–130.
- Litvak, M., Miller, S., Wofsy, S., & Goulden, M. L. (2003). Effect of stand age on whole ecosystem CO<sub>2</sub> exchange in Canadian boreal forest. *Journal of Geophysical Research*, 108(D3), Art No. 8225.
- Liu, J., Chen, J. M., Cihlar, J., & Chen, W. (1999). Net primary productivity distribution in the BOREAS region from a process model using satellite and surface data. *Journal of Geophysical Research*, 104(D22), 27735–27754.
- Loechel, S. E., Walthall, C. L., de Colstoun, E. B., Chen, J., Markham, B. L., & Miller, J. (1997). Variability of boreal forest reflectances as measured from a helicopter platform. *Journal of Geophysical Research*, 102(D24), 29495–29504.
- Middleton, E. M., Sullivan, J. H., Bovard, B. D., DeLuca, A. J., Chan, S. S., & Cannon, T. A. (1997). Seasonal variability in foliar characteristics and physiology for boreal forest species at the five Saskatchewan tower sites during the 1994 boreal Ecosystem–Atmosphere Study (BOREAS). *Journal of Geophysical Research*, 102(D24), 28831–28844.
- Miller, J. R., White, H. P., Chen, J. M., Peddle, D. R., McDermid, G., Fournier, R. A., Shepherd, P., Rubinstein, I., Freemantle, J., Soffer, R., & LeDrew, E. (1997). Seasonal change in understory reflectance of boreal forests and influence on canopy vegetation indices. *Journal of Geophysical Research*, 102(D24), 29475–29482.
- Moghaddam, M., & Saatchi, S. (1999). Monitoring tree moisture using an estimation algorithm applied to SAR data from BOREAS. *IEEE Transactions on Geoscience and Remote Sensing*, 37(2), 901–916.
- Moghaddam, M., Saatchi, S., & Cuenca, R. H. (2000). Estimating subcanopy soil moisture with radar. *Journal of Geophysical Research*, 105 (D11), 14899–14911.
- Moncreiff, J. B., Malhi, Y., & Leuning, R. (1996). The propagation of errors in long-term measurements of land-atmosphere fluxes of carbon and water. *Global Change Biology*, 2, 231–240.
- Moosavi, S. C., & Crill, P. M. (1997). Controls on CH<sub>4</sub> and CO<sub>2</sub> emissions along two moisture gradients in the Canadian boreal zone. *Journal of Geophysical Research*, 102(D24), 29261–29277.
- Myneni, R. B., Hoffman, S., Knyazikhin, Y., Privette, J. L., Glassy, J., Tian, Y., Wang, Y., Song, X., Zhang, Y., Smith, G. R., Lott, A., Friedl, M., Morisette, J. T., Votava, P., Nemani, R. R., & Running, S. W. (2002). Global products of vegetation leaf area and fraction absorbed PAR from year one of MODIS data. *Remote Sensing of Environment*, 83, 214–231.
- Myneni, R. B., Keeling, C. D., Tucker, C. J., Asrar, G., & Nemani, R. R. (1997). Increased plant growth in the northern high latitudes from 1981 to 1991. *Nature*, 386(6626), 698–702.
- Newcomer, J. A., Huemmrich, K. F., Landis, D., Nickeson, J., Conrad, S., Knapp, D., Curd, S., Morrell, A., Hodkinson, D., Nelson, E., Cihlar, J., Margolis, H., Goodison, B., Hall, F., & Sellers, P. (2001). Managing and supporting large integrated and interdisciplinary field studies: The BOREAS example. *Journal of Geophysical Research*, 106(D24), 33517–33528.
- Nichol, C. J., Huemmrich, K. F., Black, T. A., Jarvis, P. G., Walthall, C. L., Grace, J., & Hall, F. G. (2000). Remote sensing of photosynthetic-light-use efficiency of boreal forest. *Agricultural and Forest Meteorology*, 101, 131–142.
- Nobel, P. S., & Long, S. P. (1985). Canopy structure and light interception. In: J. Coombs, D. O. Hall, S. P. Long, & J. M. O. Scurlock (Eds.), *Techniques in bioproductivity and photosynthesis* (2nd ed.). Oxford: Pergamon.
- North, P. R. J. (1996). Three-dimensional forest light interaction model using a Monte Carlo method. *IEEE Transactions on Geoscience and Remote Sensing*, 34(4), 946–956.
- Ogunjemiyo, S. O., Schuepp, P. H., Desjardins, R. L., & MacPherson, J. I. (1997). Analysis of flux maps vs. surface characteristics from Twin Otter grid flights in BOREAS 1994. *Journal of Geophysical Research*, 102(D24), 29135–29146.
- Peddle, D. R. (1995). Knowledge formulation for supervised evidential classification. *Photogrammetric Engineering and Remote Sensing*, 61(4), 409–417.
- Peddle, D. R. (1999). Integration of a geometric optical reflectance model with an evidential reasoning image classifier for improved forest information extraction. *Canadian Journal of Remote Sensing. Special Issue on Remote Sensing Models and Image Processing*, 25 (2), 189–196.
- Peddle, D. R., Franklin, S. E., Johnson, R. L., Lavigne, M. A., & Wulder, M. A. (2003). Structural change detection in a disturbed conifer forest using a geometric optical reflectance model in Multiple-Forward Mode. *IEEE Transactions on Geoscience and Remote Sensing*, 41(1), 163–166.
- Peddle, D. R., Hall, F. G., & LeDrew, E. F. (1999). Spectral mixture analysis and geometric optical reflectance modeling of boreal forest biophysical structure. *Remote Sensing of Environment*, 67(3), 288–297.
- Peddle, D. R., Hall, F. G., LeDrew, E. F., & Knapp, D. E. (1997). Classification of forest land cover in BOREAS. II: Comparison of results from a sub-pixel scale physical modeling approach and a training based method. *Canadian Journal of Remote Sensing. BOREAS Special Issue*, 23(2), 131–142.
- Peddle, D. R., Johnson, R. L., Cihlar, J., & Latifovic, R. (2003). Large area forest classification and biophysical parameter estimation using the 5-Scale canopy reflectance model in Multiple-Forward Mode. *Remote Sensing of Environment*, 89, 252–263 (this issue).
- Peddle, D. R., Johnson, R. L., Cihlar, J., Leblanc, S. G., & Chen, J. M. (2003). MFM-5-Scale: A physically-based inversion modeling approach for unsupervised cluster labeling and independent forest land-cover classification. *Canadian Journal of Remote Sensing* (in press).
- Peddle, D. R., White, H. P., Soffer, R. J., Miller, J. R., & LeDrew, E. F. (2001). Reflectance processing of remote sensing spectroradiometer data in BOREAS. *Computers and Geosciences*, 27, 203–213.
- Pitman, A. J., & Henderson-Sellers, A. (1998). Recent progress and results from the project for inter-comparison of land-surface parameterization schemes. *Journal of Hydrology*, 213, 128–135.
- Pomeroy, J. W., Parviainen, J., Hedstrom, N., & Gray, D. M. (1998). Coupled modeling of forest snow interception and sublimation. *Hydrological Processes*, 12, 2317–2337.
- Pomeroy, J. W., & Schmidt, R. A. (1993). The use of fractal geometry in modeling intercepted snow accumulation and sublimation. *Canadian Journal of Forest Research*, 20, 1250–1253.
- Potter, C. S., Coughlin, J. C., & Brooks, V. (1999). Investigations of BOREAS spatial data in support of regional ecosystem modeling. *Journal of Geophysical Research*, 104(D22), 27771–27788.
- Potter, C. S., Wang, S., Nikolov, N. T., McGuire, A. D., Liu, J., King, A. S., Kimball, J. S., Grant, R. F., Frolking, S. E., Clein, J. S., Chen, J. M., & Amthor, J. S. (2001). Comparison of boreal ecosystem model sensitivity to variability in climate and forest site parameters. *Journal of Geophysical Research*, 106, 33671–33687.
- Privette, J. L., Eck, T. F., & Deering, D. W. (1997). Estimating spectral albedo and nadir reflectance through inversion of simple BDRF models with AVHRR/MODIS-like data. *Journal of Geophysical Research*, 102, 29529–29542.
- Rahman, A. F., Gamon, J. A., Fuentes, D. A., Roberts, D. A., & Prentiss, D. (2001). Modeling spatially distributed ecosystem flux of boreal forests using hyperspectral indices from AVIRIS imagery. *Journal of Geophysical Research*, 106(D24), 33579–33591.
- Ranson, K. J., & Sun, G. (2000). Effects of environmental conditions on boreal forest classification and biomass estimates with SAR. *IEEE Transactions on Geoscience and Remote Sensing*, 38, 1242–1252.
- Ranson, K. J., Sun, G., Lang, R., Chauhan, N., Cacciola, R., & Kilic, O. (1997). Mapping boreal forest biomass from spaceborne synthetic aperture radar. *Journal of Geophysical Research*, 102 (D24), 29599–29610.
- Raplee, G., Steyaert, L. T., & Hall, F. G. (2001). Moss and lichen cover mapping at local and regional scales in the boreal forest ecosystem of central Canada. *Journal of Geophysical Research*, 106(D24), 33551–33563.
- Rosema, A., Verhoef, W., Noorbergen, H., & Borgesius, J. (1992). A new



- light interaction model in support of forest monitoring. *Remote Sensing of Environment*, 42, 23–41.
- Running, S. W., & Coughlan, J. C. (1988). A general model of forest ecosystem processes for regional applications: 1. Hydrologic balance, canopy gas exchange and primary production processes. *Ecological Modelling*, 42, 125–154.
- Russell, C. A., Irons, J. R., & Dabney, P. W. (1997). Bidirectional reflectance of selected BOREAS sites from multiangle airborne data. *Journal of Geophysical Research*, 102(D24), 29505–29516.
- Ryan, M. G., & Yoder, B. J. (1997). Hydraulic limits to tree height and tree growth. *BioScience*, 47, 235–242.
- Saatchi, S., & Moghaddam, M. (2000). Estimation of crown and stem water content and biomass of boreal forest using polarimetric SAR imagery. *IEEE Transactions on Geoscience and Remote Sensing*, 38, 697–709.
- Sandmeier, S. T., & Deering, D. W. (1999). Structure analysis and classification of boreal forests using airborne hyperspectral BRDF data from ASAS. *Remote Sensing of Environment*, 69, 281–295.
- Sellers, P., Hall, F., Kelly, R., Black, A., Baldocchi, D., Berry, J., Ryan, M., Ranson, K. J., Crill, P., Lettenmaier, D., Margolis, H., Cihlar, J., Newcomer, J., Fitzjarrald, D., Jarvis, P., Gower, S. T., Halliwell, D., Williams, D., Goodison, B., Wickland, D., & Guertin, F. (1997). BOREAS in 1997: Experiment overview, scientific results, and future directions. *Journal of Geophysical Research*, 102(D24), 28731–28769.
- Sellers, P., Hall, F., Margolis, H., Kelly, B., Baldocchi, D., den Hartog, G., Cihlar, J., Ryan, M. G., Goodison, B., Crill, P., Ranson, J., Lettenmaier, D., & Wickland, D. E. (1995). The Boreal Ecosystem–Atmosphere Study (BOREAS): An overview and early results from the 1994 field year. *Bulletin of the American Meteorological Society*, 76(9), 1549–1577.
- Sellers, P. J., Hall, F. G., Baldocchi, D., Cihlar, J., Crill, P., Den Hartog, J., Goodison, B., Kelly, R. D., Lettenmaier, D., Margolis, H., Ranson, J., & Ryan, M. (1994). *BOREAS Experiment Plan, Version 3.0*. May 1994. NASA Goddard Space Flight Center, Greenbelt, MD. 4 volumes, variously paged.
- Serrano, L., Gamon, J. A., & Berry, J. (1997). Estimation of leaf area with an integrating sphere. *Tree Physiology*, 17, 571–576.
- Sims, D. A., & Gamon, J. A. (2002). Relationships between leaf pigment content and spectral reflectance across a wide range of species, leaf structures and developmental stages. *Remote Sensing of Environment*, 81, 337–354.
- Steyaert, L. T., Hall, F. G., & Loveland, T. R. (1997). Land cover mapping, fire regeneration, and scaling studies in the Canadian boreal forest with 1 km AVHRR and Landsat TM data. *Journal of Geophysical Research*, 102(D24), 29581–29598.
- Stylinski, C. D., Gamon, J. A., & Oechel, W. C. (2002). Seasonal patterns of reflectance indices, carotenoid pigments and photosynthesis of evergreen chaparral species. *Oecologia*, 131, 366–374.
- Treuhaft, R. N., Asner, G. P., Law, B. E., & vanTuyl, S. (2002). Forest leaf area density profiles from the quantitative fusion of radar and hyperspectral data. *Journal of Geophysical Research*, 107(D21), 4568 (doi:10.1029/2001JD000646).
- Treuhaft, R. N., & Siqueira, P. R. (2000). Vertical structure of vegetated land surfaces from interferometric and polarimetric radar. *Radio Science*, 35, 141–177.
- Tucker, C. J., Slayback, D. A., Pinzon, J. E., Los, S. O., Myneni, R. B., & Taylor, M. G. (2001). Higher northern latitude NDVI and growing season trends from 1982 to 1999. *International Journal of Biometeorology*, 45, 184–190.
- Vanderbilt, V. C., Perry, G. L., Livingston, G. P., Ustin, S. L., Diaz Barrios, M. C., Bréon, F. M., Leroy, M., Balois, J. Y., Morrissey, L. R., Shewchuk, S. R., Stearn, J. A., Zedler, S. E., Syder, J. L., Bouffières, S., & Herman, M. (2002). Inundation discriminated using sun glint. *IEEE Transactions on Geoscience and Remote Sensing*, 40, 1279–1286.
- Viterbo, P., & Betts, A. K. (1999). Impact on ECMWF forecasts of changes to the albedo of the boreal forests in the presence of snow. *Journal of Geophysical Research*, 104, 27803–27810.
- Walthall, C. L., Loebel, S. E., Huemmrich, K. F., Brown de Colstoun, E., Chen, J., Markham, B. L., Miller, J., & Walter-Shea, E. A. (1997, April 7–11). Spectral information content of the boreal forest. In G. Guyot, & T. Phulpin (Eds.), *Proceedings of Physical Measures and Signatures in Remote Sensing* (pp. 607–611). France: Courchevel.
- Walthall, C. L., Williams, D. L., Dykes, W., & Young, D. C. (2001). Principles of helicopters as platforms for optical wavelength remote sensing: The NASA GSFC/WFF helicopter remote sensing system. *Remote Sensing Reviews*, 18(2–4), 83–102.
- Way, J. B., Zimmermann, R., Rignot, E., McDonald, K., & Oren, R. (1997). Winter and spring thaw as observed with imaging radar at BOREAS. *Journal of Geophysical Research*, 102(D24), 29673–29684.
- White, H. P., Miller, J. R., & Chen, J. M. (2001). Four-scale linear model for anisotropic reflectance (FLAIR) for plant canopies: Part I. Model description and partial validation. *IEEE Transactions in Geosciences and Remote Sensing*, 39(5), 1072–1083.
- White, H. P., Miller, J. R., & Chen, J. M. (2002). Four-Scale Linear Model for Anisotropic Reflectance (FLAIR) for plant canopies: II. Validation and inversion with CASI, POLDER, and PARABOLA data at BOREAS. *IEEE Transactions in Geosciences and Remote Sensing*, 40(5), 1038–1046.
- Yoder, B. J., Ryan, M. F., Waring, R., Schoettle, A. W., & Kaufmann, M. R. (1994). Evidence of reduced photosynthetic rates in old trees. *Forest Science*, 40(3), 513–527.
- Zarco-Tejada, P. J., & Miller, J. R. (1999). Land cover mapping at BOREAS using red edge spectral parameters from CASI imagery. *Journal of Geophysical Research*, 104(D22), 27921–27933.
- Zarco-Tejada, P. J., Miller, J. R., Harron, J., Hu, B., Noland, T. L., Goel, N., Mohammed, G. H., & Sampson, P. (2003). Needle chlorophyll content estimation through model inversion using hyperspectral data from boreal conifer forest canopies. *Remote Sensing of Environment*, 89, 189–199 (this issue).